SCIENCE CHINA
Information Sciences

• REVIEW •

June 2018, Vol. 61 060410:1–060410:27
https://doi.org/10.1007/s11432-018-9442-3

Special Focus on Flexible Electronics Technology

Review on flexible photonics/electronics integrated devices and fabrication strategy

Shisheng CAI[1,2], Zhiyuan HAN[1,2], Fengle WANG[1,2], Kunwei ZHENG[1,2], Yu CAO[1,2], Yinji MA[1,2] & Xue FENG[1,2*]

[1]*Applied Mechanics Laboratory, Department of Engineering Mechanics, Tsinghua University, Beijing* 100084*, China;*
[2]*Interdisciplinary Research Center for Flexible Electronics Technology, Tsinghua University, Beijing* 100084*, China*

Received 27 March 2018/Accepted 26 April 2018/Published online 15 May 2018

Abstract In recent years, to meet the greater demand for next generation electronic devices that are transplantable, lightweight and portable, flexible and large-scale integrated electronics attract much more attention have been of interest in both industry and academia. Organic electronics and stretchable inorganic electronics are the two major branches of flexible electronics. With the semiconductive and flexible properties of the organic semiconductor materials, flexible organic electronics have become a mainstay of our technology. Compared to organic electronics, stretchable and flexible inorganic electronics are fabricated via mechanical design with inorganic electronic components on flexible substrates, which have stretchability and flexibility to enable very large deformations without degradation of performance. This review summarizes the recent progress on fabrication strategies, such as hydrodynamic organic nanowire printing and inkjet-assisted nanotransfer printing of flexible organic electronics, and screen printing, soft lithography and transfer printing of flexible inorganic electronics. In addition, this review considers large-scale organic and inorganic flexible electronic systems and the future applications of flexible and stretchable electronics.

Keywords flexible and stretchable electronics, organic photonics/electronics, inorganic photonics/electronics, fabrication strategies, flexible electronic system

Citation Cai S S, Han Z Y, Wang F L, et al. Review on flexible photonics/electronics integrated devices and fabrication strategy. Sci China Inf Sci, 2018, 61(6): 060410, https://doi.org/10.1007/s11432-018-9442-3

1 Introduction

Over last decade, studies have provide routes for fabricating flexible electronic systems which can be bent, twisted, folded, stretched, and conformally wrapped onto arbitrarily curved surfaces without significant changes in their characteristics [1–10]. Compared to traditional semiconductor devices, flexible electronics are not the rigid, brittle and planar to enable new applications, such as E-skin devices for diagnosis and treatment [11–18], wearable devices [2, 7, 11, 19–21], flexible display [22–25], implantable devices [26, 27], and so on. In recent years, because of the excellent performance of flexible electronics, they have attracted much more attention [28–30] in both industry and academia, such as Harvard, UIUC, IBM, Intel, where the work includes development of flexible solar cells to, light-emitting diodes, lasers, photodetectors, digital imaging system, Field Effect Transistor (FET) array, transient circuits, and epidermal devices.

Flexible electronics originate from organic electronics. Figure 1 shows a brief timeline of the development of flexible electronics based on organic semiconductor materials and stretchable and flexible

* Corresponding author (email: fengxue@tsinghua.edu.cn)

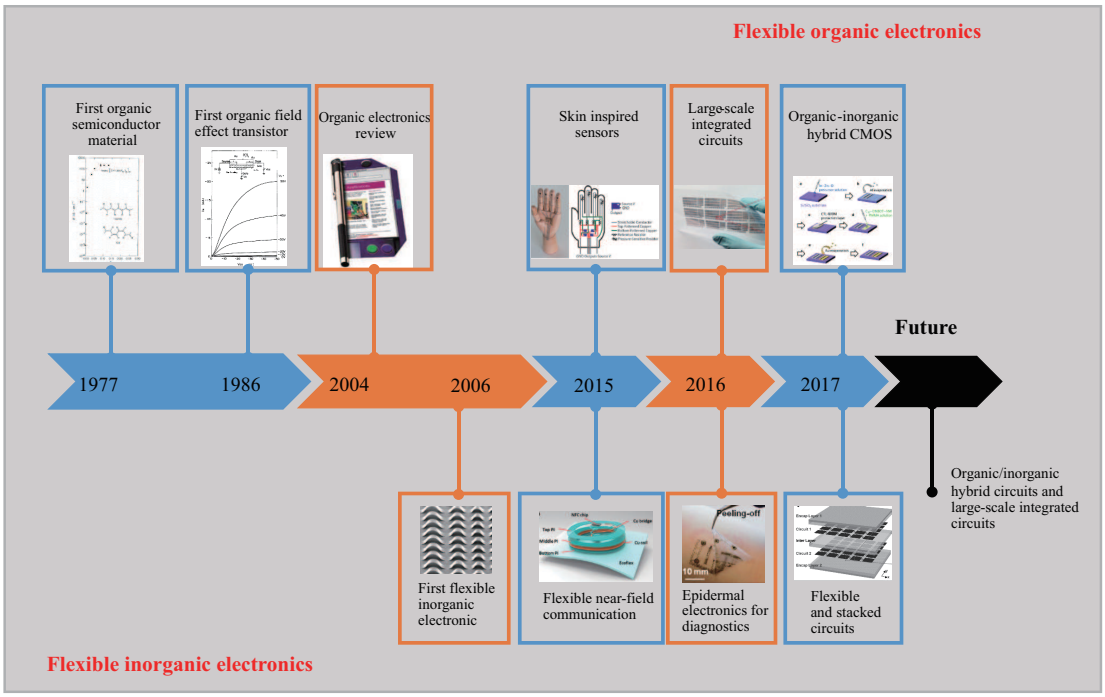

Figure 1 (Color online) A brief timeline of the development of flexible electronics based on organic semiconductor materials and stretchable and flexible inorganic devices: first organic semiconductor material [31] @Copyright 1977 American Physical Society; first organic field effect transistor [32] @Copyright 1986 American Institute of Physics; organic electronics review [33] @Copyright 2004 Springer Nature; skin inspired sensors [34] @Copyright 2015 American Association for the Advancement of Science; large-scale integrated circuits [35] @Copyright 2016 John Wiley and Sons; organic-inorganic hybrid CMOS [36] @Copyright 2017 Elsevier B.V; first flexible inorganic electronic [37] @Copyright 2006 Springer Nature; flexible near-field communication [38] @Copyright 2014 John Wiley and Sons; epidermal electronics for diagnostics [39] @Copyright 2015 John Wiley and Sons; flexible and stacked circuits [40] @Copyright 2016 John Wiley and Sons.

inorganic devices. Because organic semiconductors are compatible with flexible substrates and conducting polymers, there have been efforts to replace silicon with organic semiconductor to obtain the flexible electronics. The first organic semiconductor material [31], organic field effect transistor [32], and organic light-emitting diode [41] were presented respectively in 1977, 1986, and 1987. Afterwards, to satisfy high-performance requirements of large-scale integrated circuits, many different p-type and n-type conducting organic materials [42–44] such as pentacene and polyphenylene vinylene (PPV), were synthesized. In 2004, Forrest [33], a well-known microelectronics scientist at Princeton University, considered the status and development of organic electronics and presented conceptual design and conceptual manufacturing methods, which promoted the rapid development of organic flexible electronics. Since progress in organic semiconductors has risen steadily, attempts to develop integrated systems consisting of organic field effect transistor (OFET) [45–48] and the functional groups [49] have been made to produce an independent system in the last five years.

Compared to organic electronics, stretchable and flexible inorganic electronics were fabricated with inorganic electronic components on flexible substrates via mechanical design, which was first reported on by Rogers et al. in 2006 [37]. Ultrathin semiconductor nanoribbons were transferred onto pre-strained polydimethylsiloxane (PDMS) to obtain the buckling electronics with extremely high levels of stretchability, compressibility, and bendability. Since 2006, more and more attention has been focused on inorganic island, "wavy" structural configurations design [50–54] and transfer printing strategy [55–61] which promote the development of large-scale and flexible inorganic electronics. Because of their stretchability, flexibility and semiconductor properties, various types of flexible inorganic electronics have been assembled in recent years and, to enable wider applications and to have more varied working forms, these integrated devices could be optimized.

This review comprises as follows. Section 2 provides a comprehensive overview of flexible fabrication

methods which are divided into two aspects: hydrodynamic organic nanowire printing and inkjet-assisted nanotransfer printing technique of flexible organic electronics, and screen printing, soft lithography and transfer printing of flexible inorganic electronics. Section 3 deals with representative applications of flexible organic field-effect transistors, flexible organic lighting diodes and flexible organic electronic system on a large scale. Section 4 demonstrates representative applications of stretchable and flexible inorganic electronics on a large-scale. Finally, we present some current challenges, comparisons and future directions for organic and inorganic flexible electronics.

2 Fabrication strategies of flexible integrated electronics on a large scale

2.1 The method of fabricating flexible and organic integrated electronics on a large scale

In semiconductor device fabrication, silicon monolithic integrated circuits can be fabricated in a large area, such as integration of transistors, capacitors, resistors, and corresponding interconnects [62]. However, organic materials for organic electronic devices are not compatible with the single-material monolithic integration, since the functional components requiring different organic materials. The organic materials have many advantages, including natural flexibility and low cost [63–65]. The development of an efficient way to produce large-scale organic integrated electronics is urgent.

The traditional way to fabricate organic electronics is by spin coating [66] or evaporation [67]. In the OFETs made by Sheng, Cytop layer was spin-coated onto the AlOx:Nd layer and the pentacene film was thermally evaporated onto the insulator under a vacuum pressure of $\sim 3 \times 10^{-4}$ Pa with a deposition rate of 0.1 Å s^{-1} [67]. The OFETs modified by Cytop exhibited better electric characteristics than the one without Cytop. The active organic material of Oren's OFETs was spin coated on to the substrate. The PII2T-Si chosen as the organic semiconductor was dissolved in chloroform and heated to 58°C, stirred 20 min and spin-coated onto the gate electrode at 1000 rpm for 60 s. By using the PII2T-Si polymer, the OFETs demonstrated stable performance in aqueous environments (DI water and seawater). Wang et al. [66] fabricated an organic flexible transistor with silk fibroin as the gate dielectric. A silk fibroin thin film of 30 nm thickness was applied onto the poly (ethylene terephthalate) (PET) substrate by spin coating and the pentacene was deposited on the dielectric layer by thermal evaporation. Owing to the silk fibroin film, the amorphous phase was reduced and the orthorhombic phase was increased, which resulted in a high field-effect mobility. Many other studies [68] based on spin coating or evaporation, are considered here, though these could also integrate with large-scale electronics.

Floating film transfer method (FTM) is a modified spin coating process. Pandey et al. [69] demonstrated that judicious selection of solvents with high boiling point or low boiling point during FTM could result in static casting (S-FTM) or dynamic casting (D-FTM). As Figure 2(a) (left) shows, PBTTT-C14/chlorobenzene solution spread throughout the entire surface of the substrate, forming floating-film after the slow evaporation of chlorobenzene in the S-FTM processing. As for D-FTM, PBTTT-C14/$CHCl_3$ spread in all of directions in branched form like a star-fish followed by simultaneous solidification leading to the formation of oriented floating-films. The X-ray diffraction measurement revealed that D-FTM film had relatively extended π-conjugation length compared to the S-FTM film. Meanwhile the field-effect mobility of OFETs fabricated with D-FTM films in parallel orientation was high compared to that prepared by both of the S-FTM and perpendicular D-FTM films, as Figure 2(a) (right) shows; also in addition, and the high mobility was as good as that achieved by spin coating with high boiling solvents followed by annealing [70, 71]. Therefore, the FTM is a more promising strategy to fabricate film used for flexible organic electronics than the traditional spin-coating and drop casting methods [69].

Min et al. [49] demonstrated a new technique to fabricate organic electronics based on jet printing technology [72] and electrospinning [73,74]. The hydrodynamic organic nanowire (ONW) printing (ONP) technique was able to print highly aligned and individually controlled organic semiconducting nanowires (OSNWs) at desired positions. The aligned ONWs were used as a shadow mask to make large-scale nanopatterns to fabricate OSNW transistor arrays, complementary inverter arrays and p-type/n-type polymer semiconductor NWs. Organic nanowire lithography (ONWL) is a potential technique to replace E-beam

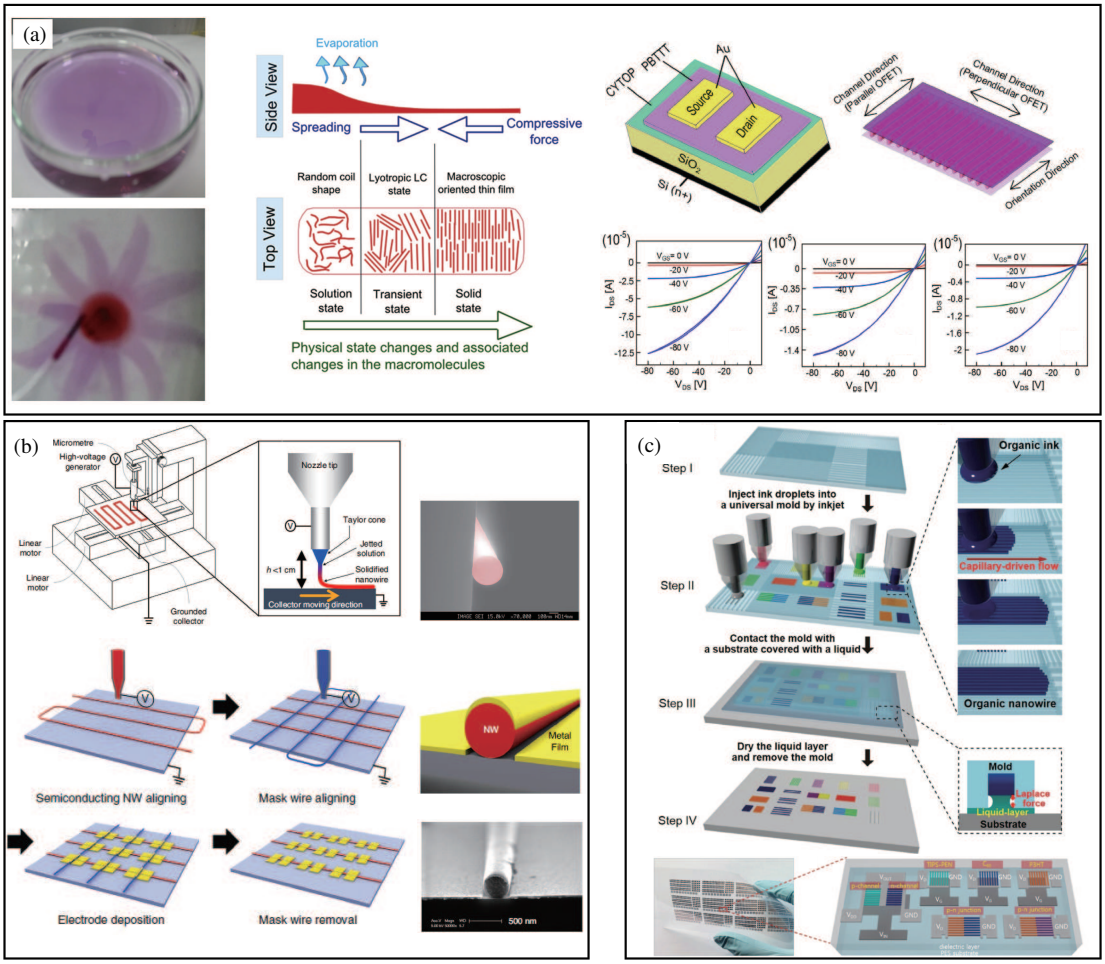

Figure 2 (Color online) The method of fabricating large-scale organic electronics. (a) Photograph of the thin films formed at liquid substrate using S-FTM and D-FTM, and schematic for possible mechanism for macroscope orientation in D-FTM (left); device configuration of the fabricated OFET and output OFET characteristics of PBTTT-C14 films prepared by D-FTM parallel, D-FTM perpendicular and S-FTM (right) [69] @Copyright 2017 Elsevier B.V. (b) Schematic diagram of the home-built ONW printer and NW printing process. Field emission scanning electron microscope image showing cross section of well-aligned polyvinylcabazol (PVK) NW, which forms a perfect circle (top); schematic illustration of the process to fabricate organic FET with nanoscale channel length and channel width and scanning electron microscope images of P3TH:PEO-blend NW and nano-sized electrode gap (down) [49] @Copyright 2013 Springer Nature. And (c) schematic illustration of the inkjet-NTP process and schematic illustration of an ink droplet filling the recessed nanochannels of a selected area of the mold through capillary-driven flow. Schematic illustration of a liquid bridge formed by a polar liquid layer between the nanowires and a substrate (inset); a photographic image of the large-scale integrated electronic devices composed of FET, inverter, and p-n diode arrays made of single-crystal organic nanowires [35] @Copyright 2016 John Wiley and Sons.

lithography, which is relatively slow, complicated and expensive. As Figure 2(b) (top) shows, the ONW printer consisted of a high-speed linear motor the x-y stage, a flat grounded collector, a micrometer to control the tip-to-collector distance, a syringe pump, a nozzle and a high-voltage generator. The ONWs were printed from the nozzle tip through the high electric effect, similar to electrospinning. To get the aligned ONWs, they adjusted x-y stage when the NWs were ejected. They printed polyvinylcabazol (PVK) NWs on a substrate, followed by deposition of metal films. Then the ONWs were removed by adhesive tape, detachment or sonication. Finally aligned nano-gaps were achieved successfully, and the patterns could be used to fabricate organic transistors and complementary circuit arrays. P3HT:PEO-blend NWs were printed between source and drain electrodes to form the OFET with good electric performance. The ONWP is a promising approach for the fabrication of large-scale flexible organic integrated circuits [49]. However this technique has limitations, the initial material must have high

viscosity and the printing patterns have the unwanted polymer residues. An ideal printing method to produce flexible organic electronics can be used to precisely control the morphology and crystallinity of various organic materials. Park and coworkers [35] developed a nanotransfer printing technique to produce large-scale nanowire arrays with controlled orientation and crystallinity. The method was able to fabricate heterogeneous monolithic integration of various patterns with different organic functional materials on a single substrate. It was based on a combination of inkjet printing [75] and nanotransfer printing via a liquid-bridge-mediated transfer process, called inkjet-assisted nanotransfer printing (inkjet-NTP) [76]. Figure 2(c) (top) shows the schematic inkjet-NTP process. First, a universal mold, which had nanoscale line patterns and was produced by using UV-assisted double replica molding, was needed. Then, various organic functional materials were deposited onto the specific position above the mold. After drying, the crystalline nanowire with the mold was taken to contact with a substrate surface, which was covered by a thin polar liquid layer. Finally, the mold was taken away from the substrate to leave the specific patterned nanowire on the substrate. In the printing process, the length of the nanowires was increased with the number of droplets and the number of the nanowires was increased with the volume of a single droplet. The most prominent content was that three different organic functional materials, including TIPS-PEN, P3HT, and fullerene (C60), were printed onto a single substrate to form the nanopatterned heterojunction. In addition, a large-scale integrated organic circuit was fabricated on a 5×10 cm^2 flexible substrate. The organic circuit consisted of field-effect transistors, complementary inverters used for driving electronic circuits and p-n diodes as photodiodes and strain sensors. Figure 2(c) (down) shows the photographic image and the schematic diagram of the integrated circuit. The research [35] demonstrated that the inkjet-NTP method is an excellent technique to integrate various functional electronics on a single chip and it is an efficient way to integrate with flexible electronics.

2.2 The method of fabricating flexible and inorganic integrated electronics on large scale

2.2.1 *Screen printing*

Screen printing is the most widely used conventional mass-printing techniques in flexible electronics due to its low capital cost, versatile pattern designs, little waste and the compatibility with a broad range of functional inks and substrates [77–79]. In this printing process ink is pressed through a patterned screen onto various substrates with a squeegee moving forward, as Figure 3(a) shows. The screen is typically made of a porous mesh, from materials such as a porous fabric or stainless steel. The fabrication of the stencil image to be replicated on the mesh is photochemical or manual. Currently, the printed line width can be 30–100 μm which mainly depends on the screen mask resolution and the quality of conductive inks/pastes [77]. In terms of throughput, edge resolution and achievable wet thickness, rotary screen printing have the best performance from all types of screen printing, as Figure 3(b) shows [80].

In recent years, there has been interest in using spherical or flake shape silver particles/nanowires and carbon-based materials, such as graphene and carbon nanotubes, in conductive screen-printing inks for flexible inorganic integrated circuits. High-resolution silver nanowire (AgNW) patterns are screen-printed on flexible PET, as Figure 3(c) shows [77]. A minimum characteristic size of the printed line width and the inter-row spacing is 50 μm. The resistance of AgNW lines for different lengths or line widths is displayed in Figure 3(d), indicating good uniformity of the printed lines, as Figure 3(d) shows. High-resolution patterning of pristine graphene was also reported by using silicon stencil, as Figure 3(e) shows [81]. The benefit of using silicon as a screen printing stencil is its excellent compatibility with photolithography, giving rise to well-defined and high-resolution stencil patterns. Both their work achieved high electrical conductivity for demonstrated patterns, showing the feasibility for flexible inorganic electronics. Screen printing is an inexpensive mass fabrication technique for the integration of various electronics onto a flexible substrate. In addition, the ink viscosity hugely influences the quality of screen-printed films, and should be critically match the mesh used in the stencil [82].

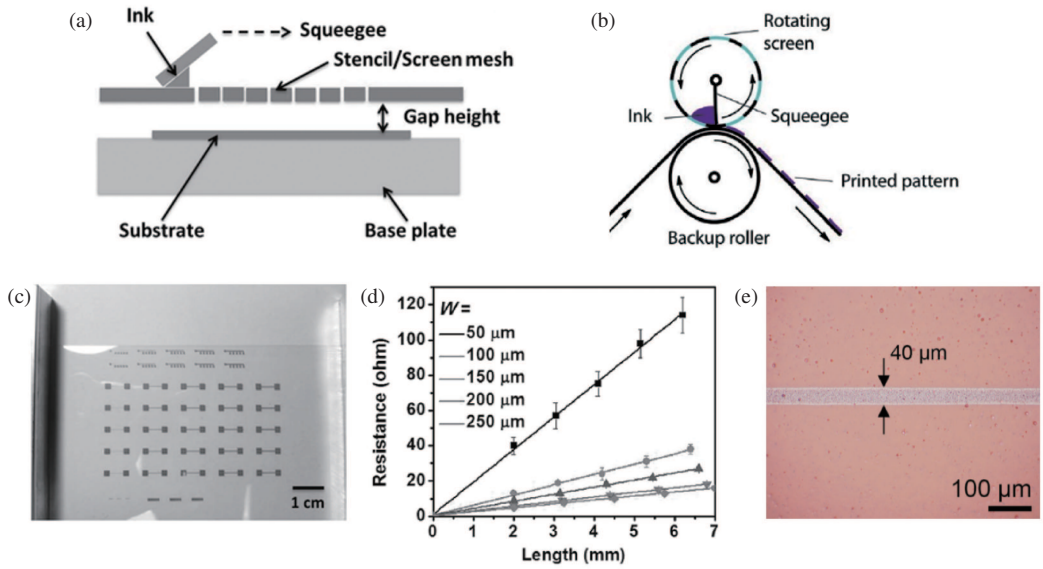

Figure 3 (Color online) (a) Scheme of the screen-printing process [77] Copyright 2016, John Wiley and Sons. (b) Rotary screen printing [80] @Copyright 2012 Elsevier Ltd. (c) Screen-printed AgNW patterns on flexible PET substrate [77] @Copyright 2016 John Wiley and Sons. (d) Measured resistance of the screen-printed AgNW lines at different length and with various line widths [77] @Copyright 2016 John Wiley and Sons. (e) Screen-printed graphene line with the width of 40 μm [81] @Copyright 2014 John Wiley and Sons.

2.2.2 *Soft lithography*

Another fabrication method of flexible printed electronics, soft lithography, is a collection of techniques for patterning substrates with an elastomeric stamp from the micro- to nanoscale [83]. The patterns are fabricated through printing inks, embossing microstructures, and replica molding with a large number of techniques such as microcontact printing (μCP) [84], replica molding (REM) [85], microtransfer molding [86]. Here, microcontact printing (μCP) will be introduced because it is probably the most representative soft-lithographic technique. During the process of the technique, an elastomeric stamp (generally made of polydimethylsiloxane (PDMS)) with patterned reliefs is inked by the alkanethiol solution and then pressed against thiol-compatible surface (e.g., gold- or copper-coated substrate), as Figure 4(a) shows. A self-assembled monolayer (SAM) is rapidly formed in the conformal contact area between stamp and substrate with the transfer of the ink to the substrate. Subsequently, the patterned SAM as an etch mask is used to pattern the underlying gold or a second SAM.

A further development of soft lithography is nanoimprint lithography (NIL), regarded as one of the next generation lithography techniques due to its low-cost, high-resolution and high-efficiency for highly integrated circuits. It was first demonstrated by Chou et al. [89] in 1995, a thermal-nanoimprinting structure was obtained by using a rigid stamp made of Si, achieving the mass fabrication of large area nano-pattern. During the thermal-NIL process, the stamp is first treated by a hydrophobic SAM molecule for anti-adhesion and then pressed against a pre-coated polymer layer. In Chou's work thermal-NIL is implemented at a temperature 105°C above the glass transition temperature (Tg) of PMMA (resist). After cooling the structured sample to room temperature the stamp is released, as Figure 4(b) (left) shows. The next stage is the removal of the residual thin resist layer by plasma etching, and then the imprinted pattern is transferred into other materials. In addition, the introduction of UV-based nanoimprinting (UV-NIL) improves the control over pattern replication and residual resist layer thickness [90]. As Figure 4(b) (right) shows, the UV-curable resist is applied for more rapid UV curing instead of slow heating and cooling process in thermal-NIL. To ensure UV light passing, UV-NIL normally uses transparent stamps, such as PDMS or quartz.

During the past years, a set of NIL techniques have been developed in terms of types of substrates, resist materials and molding processes, especially semi-continuous and continuous imprinting techniques.

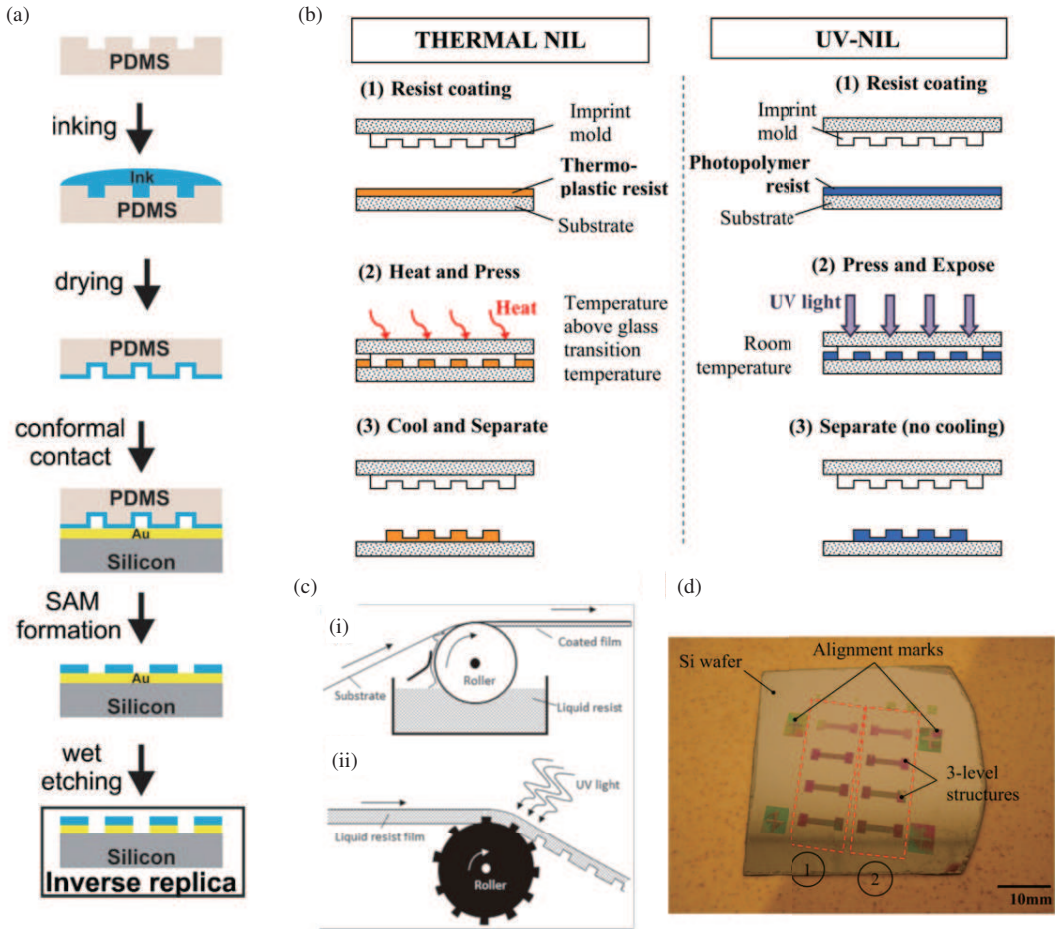

Figure 4 (Color online) (a) Fabrication steps of μCP [87] @Copyright 2009 John Wiley and Sons. (b) Comparison of a typical T-NIL and UV-NIL process [88] @Copyright 2012 IEEE. (c) Roll-to-roll UV-NIL, (i) resist coating and (ii) imprinting [89]. (d) Photograph of the 3-level patterned wafer master [88] @Copyright 2012 IEEE.

As Figure 4(c) shows, roll-to-roll ultraviolet nanoimprint lithography (R2R-UV-NIL) [91], a continuous imprinting technique, has been invented for higher process throughput and resolution. Multi-level microstructures (3-levels) with a minimum feature size of 50 μm can be continuously patterned onto a PET film as the flexible substrate by using R2R-UV-NIL technique, as Figure 4(d) shows [88]. Furthermore, the similar roll-to-plate NIL technique uses a structured roller imprinting on a rigid substrate [91].

2.2.3 *Transfer printing*

Transfer printing is an essential technique in the fabrication of flexible inorganic integrated circuits. It is well known that the inorganic semiconductor materials cannot grow directly on flexible substrates, but transfer printing technique solves the problem, enabling a technological approach to high-performance and heterointegrated circuits. The general process of transfer printing is the transfer of the inorganic film pattern from the inorganic semiconductor substrate onto flexible substrate, including pick-up and printing [57, 92]. The process of pick-up is pressing and peeling back elastomeric stamp against the inorganic semiconductor substrate which is patterned by conventional semiconductor manufacturing techniques. After that the microstructure is on the stamp and then transferred to another flexible substrate by contacting the stamp firmly onto the receiver. Transfer printing can be applied in various materials monomolecular materials (self-assembled monolayer [93], nanotubes [94], DNA [95], etc.), high-performance hard materials (single-crystal inorganic semiconductor [29], metal film [96], piezoelectric film [97, 98], etc.), and fully integrated devices (light emitting diode [99], complementary metal oxide semiconductor circuits [100],

etc.) without the condition of high temperature. Transfer printing critically depends on the control of interfacial adhesion. Researchers developed rate-dependent transfer printing for the relations between interfacial strength and interfacial fracture rate. Viscoelastic PDMS is used as the stamp, and therefore the critical energy release rate between the stamp and film is an increasing function of peel-away speed as follows [57]:

$$G_{\text{crit}}^{\text{stamp/film}}(v) = G_0 \left[1 + \left(\frac{v}{v_0}\right)^n\right],$$

where v represents peel-away speed, G_0 is the critical energy release rate when the peel-away speed approaches zero, v_0 is reference peel-away speed (when G_{crit} is the two times of G_0), and n is parameter defined by experiment. By utilizing this competitive fracture principle between the film, substrate and stamp, high peel-away speed is applied to peel the film off the original substrate while low printing speed is applied to print the film onto a flexible substrate. In addition, a microstructure-based transfer printing technique has been used to increase adhesion control by a stamp coated with microstructure, as Figure 5(a) shows [58]. A representative case of full mechanical collapse under a preload of 1 mN is shown in Figure 5(b) (retraction speed 1 mm/s), indicating an increase in stiffness as the region between the microtips collapses and contacts the substrate. As Figure 5(c) shows, laser-driven method was also used in transfer printing to realize rapid debonding of transferred chips [101]. In addition, shape memory polymers with microstructured surfaces were reported as the stamp material to replace PDMS for their shape memory property under the stimulation of heat, light or other stimuli [102]. Furthermore, a spatioselective and programmable transfer strategy via automated direct laser is presented in Figure 5(d); here, the automated direct laser wrote to trigger localized heating of a micropatterned shape memory polymer adhesion stamp to control the interfacial adhesion and complete the transfer printing [59].

3 Flexible and organic integrated electronics on a large scale

3.1 Flexible and organic field-effect transistor

Organic electronics is a promising technique for a variety of applications that require unique functionality [103]. Electronic devices, compatible with flexible electronics, are fabricated by organic materials which are usually inexpensive [104], flexible [105], and degradable [106]. Organic materials can be fabricated as light-emitting diodes [107], sensors [108], photovoltaics [109] and digital displays [110], and as multifunctional as inorganic electronics. Organic field-efficient transistors (OFETs) have been studied extensively. Here, we enumerate several representative studies about flexible OFETs. They are flexible, are low cost and are able to be fabricated on large scale, and are compatible with flexible large-scale electronics for many applications.

Recently, OFETs show prominent advantages, owing to lower cost, flexibility and compatibility with flexible electronics. Bao et al. [111] did a lot of comprehensive studies about organic OFET and applied it to flexible electronics. As organic electrons are easily damaged in humid or harsh environments, it limits the development of OFET. Bao overcame this barrier through a polyisoindigo-based polymer semiconductor with siloxane-containing solubilizing chains (PII2T-Si) semiconductor, which had a high mobility and could be spin-coated. The flexible OFETs fabricated on polyimide, a ∼40-nm-thick dielectric layer poly (4-vinylphenol)- cross-linked 4, 4′-(hexafluoroisopropylidene)-diphthalic anhydride was spin coated on the PI, followed by evaporation of gold electrodes and deposition of organic polymer deposited, as Figure 6(a) (left) shows [68]. As Figure 6(a) (right) shows, the device exhibited good electronic performance with an absence of hysteresis, an on/off ratio greater than 102 (for $\Delta V_{\text{lg}} < 400$ mV), and a subthreshold swing less than 100 mVdec^{-1}; the output characteristics (I_{sd} vs. V_{sd}) are shown in the inset. Flexible OFET was alternately exposed to DI water and seawater. Isd increased by a factor of ~ 2, upon introduction of seawater (~ 900 s). Isd decreased to the previously established baseline, when switched back to DI water (~ 1290 s). The OFETs displayed stable electrical characteristics, not only in ambient conditions but also in marine environments (DI water and seawater); however, they could be

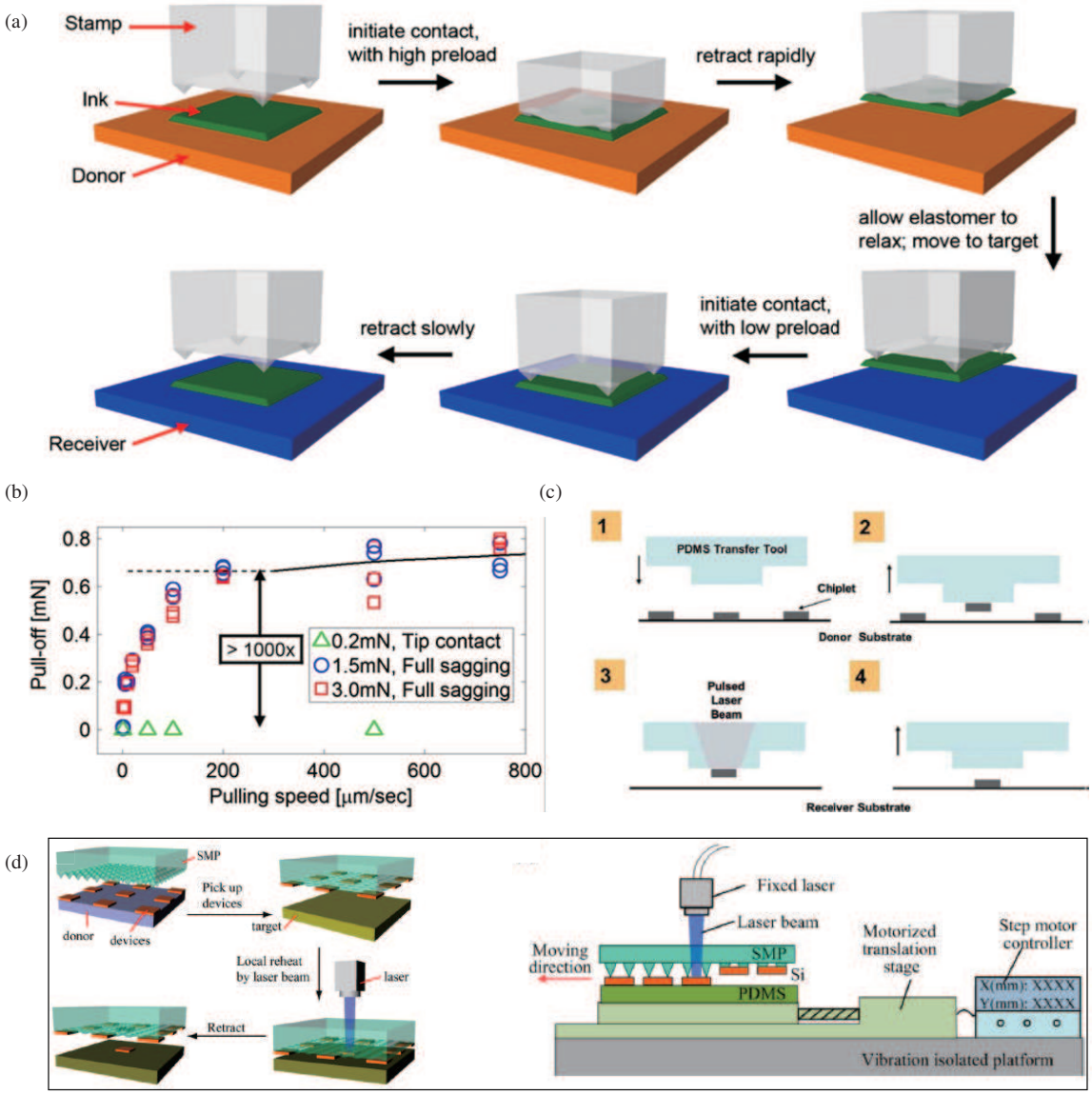

Figure 5 (Color online) (a) Transfer printing via microstructured elastomeric [58] @Copyright 2010 National Academy of Sciences; (b) adhesion test of transfer printing via microstructured elastomeric [58] @Copyright 2010 National Academy of Sciences; (c) laser-driven transfer printing [101] @Copyright 2012 IEEE; and (d) diagram of the automated printing setup [59] @Copyright 2016 American Chemical Society.

used for heavy-metal ions detection. The high yield and reproducibility indicated a promising method for large-scale integrated flexible electronics [68].

Recently, many researchers have utilized pentacene to fabricate OFET. The field-effect mobility ($\mu_{\rm FE}$) of the pentacene OFET varies from 0.5 to 4 $\rm cm^2V^{-1}s^{-1}$ and the operating voltages are in the range of -5 to -40 V [114]. Wang et al. [66] made a progress to achieve a very high $\mu_{\rm FE}$ of 23.2 $\rm cm^2V^{-1}s^{-1}$ in the saturation regime and a low operating voltage of -3 V. They used a natural biopolymer silk fibroin as the gate dielectric to fabricate the pentacene OFET. For traditional pentacene OFET, thermal evaporation can result in a combination of amorphous and crystalline forms. Silk fibroin is used to obtain the orthorhombic pentacene and to reduce amorphous phase in the pentacene fabrication process, in which the orthorhombic phase acts as the channel for carrier transport. In addition, the silk fibroin has many advantages, such as electrical insulation, optical transparency and mechanical flexibility. As Figure 6(b) (left) shows, the composition structure of the OFET PET is chosen for the flexible substrate.

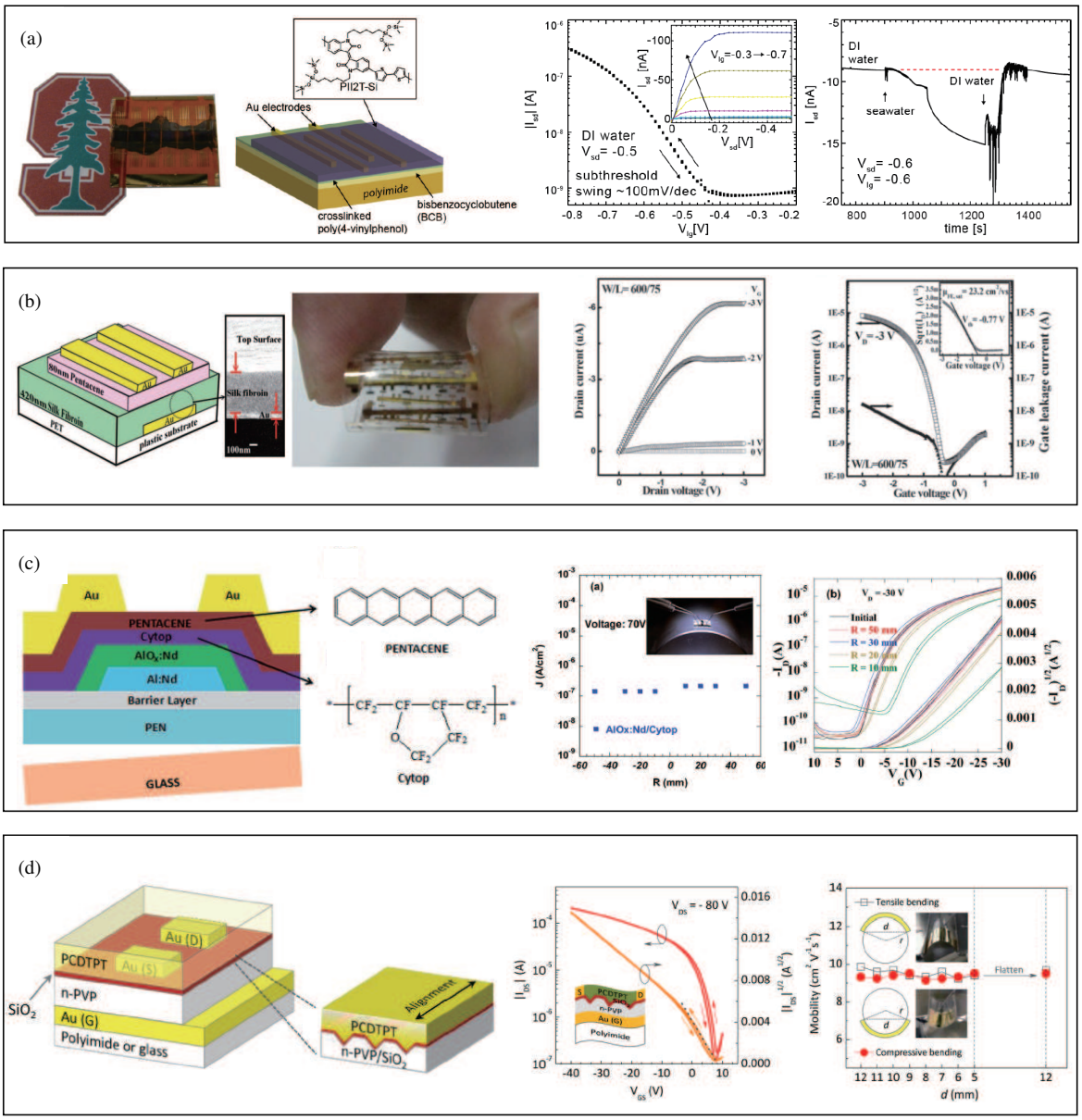

Figure 6 (Color online) Flexible OFETs. (a) Optical image and schematics of the fabricated OFET sensor on a flexible polyimide substrate (left). Transfer characteristics of $I_{\rm sd}$ vs. applied liquid-gate voltage $V_{\rm lg}$ in DI water (right). The flexible OFET is alternately exposed to DI water and seawater [68] @Copyright 2014 Springer Nature. (b) Schematic of the pentacene OTFT with silk fibroin as the gate dielectric and photograph of the rollable pentacene OTFT (left). Output characteristics, transfer and leakage current characteristics (right) [66] @Copyright 2011 John Wiley and Sons. (c) Schematic diagram of the flexible OFETs, and chemical structures of pentacene and Cytop (left). The leakage current density of AlOx:Nd/Cytop versus curvatures (middle); inset: the image of equipments in bending test. Transfer characteristics of the flexible pentacene OFET (right) under bending conditions; every curve includes forward and reverse sweeps [112] @Copyright 2015 The Royal Society of Chemistry. (d) Schematic device architecture of the flexible organic transistor with controlled nanomorphology (left). Transfer curves of the flexible device with the n-PVP/SiO_2 (2 nm) dielectric fabricated on transparent polyimide substrate (middle). Mobility plots as a function of bending distance under tensile and compressive bending stress (right) [113] @Copyright 2016 American Chemical Society.

A gate dielectric film of ∼ 420-nm-thick silk fibroin is spin coated on Au gate electrodes. Then a 70-nm-thick pentacene layer is deposited onto the dry silk fibroin film by evaporation. Finally the source and drain electrodes using Au are deposited onto the pentacene. As Figure 6(b) (right) shows, the OFET exhibited output characteristics with pinchoff and current saturation, and transfer characteristics measured at a very low frequency. The $\mu_{\rm FE,sat}$ value of 23.2 $\rm cm^2V^{-1}s^{-1}$ could be obtained by using a

Ci value of $\sim$ 30 nFcm^{-2} determined at a sweep rate of 0.25 Vs^{-1} in the quasi-static regime. Thus the OFET demonstrates the good performance of high field-effect mobility and low operating voltage and has merits of low cost, light weight and large scale. It is a promising flexible electronic device for e-paper, RFID tags or biosensors. [66]

Sun et al. [112] presented a flexible OFET with electrochemically oxidized gate insulators (AlOx:Nd) covered by a thin layer of hydroxyl-free poly (perfluorobutenylvinylether) on a flexible PEN substrate. They demonstrated that the AlOx:Nd/Cytop bilayer possessed excellent insulating characteristics with a high breakdown field, high dielectric constant, low surface roughness and low leakage current. The OFET exhibited good electrical characteristics and was stable under bending. Figure 6(c) (left) shows the schematic of the flexible OFET. They used a 300-nm-thick layer of Al-Nd (3 wt%) alloy as gate electrode and the gate metal was patterned through photolithography. By anodizing the Al-Nd film, a layer AlOx:Nd with 200 nm was fabricated as the gate insulator. Then, a 40-nm-thick hydroxyl-free poly (perfluorobutenylvinylether) commercially known as Cytop layer was spin-coated on the insulator, followed by thermally evaporating a 80-nm-thick pentacene onto the Cytop at room temperature. Finally, 50-nm-thick Au was chosen as source/drain electrodes through evaporation. Owing to the Cytop layer, the roughness of the insulator is much smoother than that without evaporating Cytop. And smooth roughness could result in better electric properties. The OFET without Cytop displays a field mobility ($\mu_{\rm FE}$) of 0.11 cm^2 V^{-1} s^{-1}, an operating voltage ($V_{\rm on}$) of -4 V, and an on/off current ratio ($I_{\rm on}/I_{\rm off}$) of $\sim 2.8\times10^5$; while the one with Cytop exhibits a higer $\mu_{\rm FE}$ of 0.75 cm^2 V^{-1} s^{-1}, a lower Von of 0 V, and a higher Ion/Ioff of $\sim 2.0\times10^5$. The flexible OFET was relatively stable under a certain degree of bending, as shown in Figure 6(c) (right), which shows the leakage current density of AlOx:Nd/Cytop vs. curvatures and transfer characteristics of the flexible pentacene OFET under bending conditions [112]. Klauk et al. [105] reported organic complementary circuits on flexible substrates. They used pentacene as the semiconductor for the *p*-channel devices and hexadecafluorocopperphthalocyanine (F_{16}CuPc) as the semiconductor for the n-channel devices to fabricate the organic thin-film transistors. A 50-nm-thick layer of polyvinylphenol was used as gate dielectric by solution processing. The OFETs and circuits were operated at supply voltages as low as 8 V.

Lee et al. [113] demonstrated OFETs with controlled nanomorphology of semiconducting polymers on chemically and mechanically stable nanogrooved polymer substrate. The nanogrooved polymer dielectrics were able to achieve high polymer alignments, as Figure 6(d) (left) shows, these yielded mobility of 19.3 and 10.5 cm^{2}V^{-1}s^{-1} on rigid and plastic substrates, respectively, and excellent bending stability of the flexible transistors. Figure 6(d) (right) shows that the flexible OFET produced a saturation hole mobility $\mu\approx10.5$ cm^{2}V^{-1}s^{-1} and mobility variations as a function of bending distance. The mobilities of OFETs are almost constant under tensile and comprehensive bending with a bending distance up to 5 mm. This study [113] is an effective method to improve electronic characteristics of OFETs by the directed self-assembly of semiconducting polymers.

3.2 Flexible and organic electronic system

Min et al. [49] performed studies on large-scale ONWL and electronics. A high-speed electrohydrodynamic organic nanowire printer was used to print large-scale organic semiconductor in a precise and controllable method. ONW FETs with a $\mu_{\rm FE}$ of 9.7 cm^{2}V^{-1}s^{-1}, high on/off current ratio ($\sim$ 106), and low contact resistance ($\sim$ 5.53 Ωcm) were fabricated in this method. Large-scale complementary inverter circuit arrays constituted by highly aligned p-type and n-type OSNWs were exhibited. P3HT blended with poly (ethylene oxide) (PEO) was used as the active material to fabricate the OSNW FETs through a hydrodynamic process. The NWs could be precisely printed between source and drain electrodes to get the p-type OFETs. They could fabricate with n-type NW FETs using a N2200:PEO-blend. Additionally PVK NWs were used to fabricate a shadow mask of the metal film through the ONW printing technique. Because the wires could be easily removed, they produced different size gaps by adjusting NW diameter. The method, called ONWL, was used to make accurate patterns on large scale and even on flexible substrates. High-capacitance ion-gel polyelectrolyte was chosen as a gate dielectric material to improve

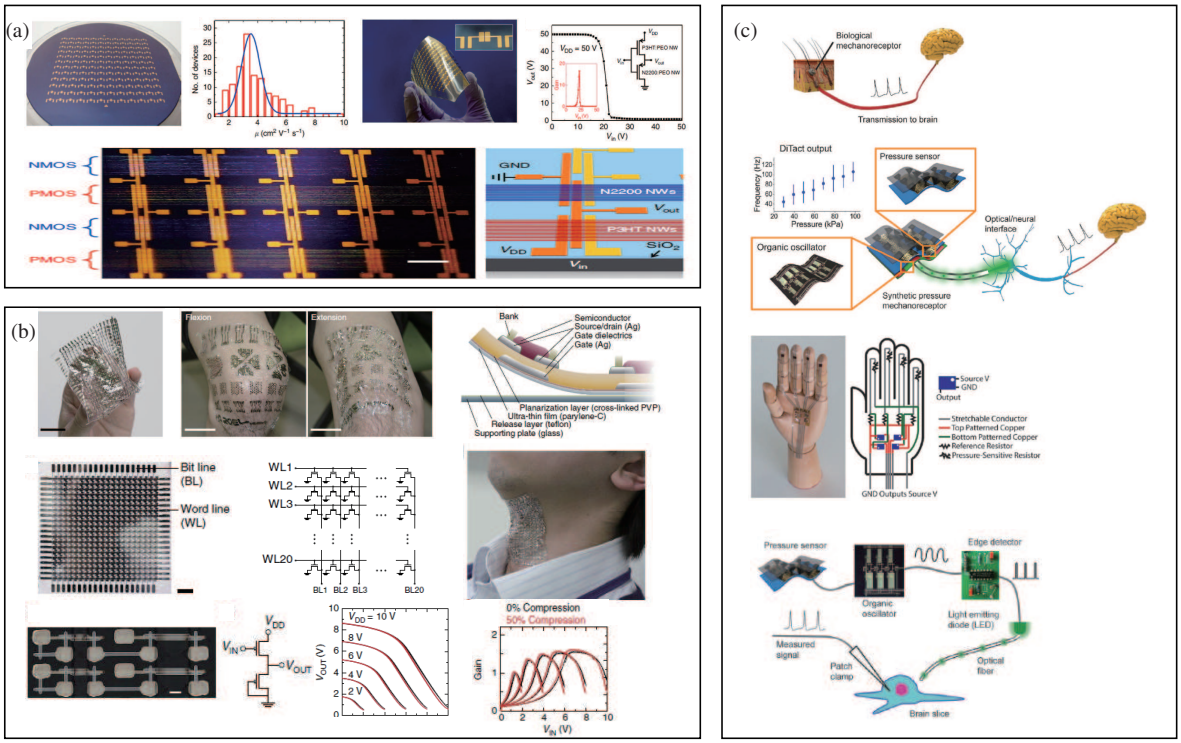

Figure 7 (Color online) Flexible organic systems on large scale. (a) Large-area single P3HT:PEO-blend NW FET array (7 cm × 7 cm) with ∼ 300 nm channel length (144 bottom-contact devices) and histogram of mobility for large-area P3HT:PEO-blend NW FET array with an average of 3.8 ± 1.6 $cm^2V^{-1}s^{-1}$. Large-area single P3HT:PEO-blend NW FET array on polyarylate (PAR) substrate and input-output voltage characteristic for complementary inverter circuit based on P3HT:PEO-blend NWs and N2200:PEO-blend NWs. Optical image of inverter array and schematic illustration of an inverter (down) [49] @Copyright 2013 Springer Nature. (b) A photograph of organic TFT devices on 1-μm-thick parylene-C films, organic device films conforming to a human knee and cross-section diagram of a thin organic TFT devices (top). Top-view photograph of a completed 10 cm × 10 cm fully printed 20 × 20 TFT array fabricated on an ultra-flexible parylene-C film, circuit diagram of the TFT array and flexible TFT array sheet conforming to a human throat (middle). Photograph of fabricated unipolar organic diode-load inverter circuits and circuit diagram of the inverter device. Static transfer characteristics of the inverter and small-signal gain as a function of input voltage (VIN). The black solid line indicates the characteristics without strain and the red solid lines indicate those of circuits under 50% compressive strain (down) [115] @Copyright 2014 Springer Nature. And (c) schematic of the function of a biological somatosensory systems, voltage pulses are generated in the skin and transported to the brain. DiTact is composed of a pressure-sensitive tactile element and an organic ring oscillator (top). Optogenetic pulses are used to stimulate live neurons. Image and circuit schematic of a model hand with DiTact sensors on the fingertips connected with stretchable interconnects (middle). Setup of the optoelectronic stimulation system for pressure-dependent neuron stimulation (down) [34] @Copyright 2015 American Association for the Advancement of Science.

the electronic characteristics. They demonstrated a large-scale (7 cm × 7 cm) NW FET array on a flexible plastic substrate (polyarylate) made up by 144 P3HT:PEO-bend FETs and a complementary inverter array using well-aligned P3HT:PEO-blend NWs and N2200:PEO-blend NWs in a short time, as illustrated in Figure 7(a) (top). A histogram of the mobility distribution showed the NW FET array with an average of 3.8 ± 1.6 $cm^2V^{-1}s^{-1}$. An optical image of the inverter array and a schematic illustration of an inverter are shown in Figure 7(a) (down). The ONWL has potential to replace E-beam lithography and a combination of ONWL with ONP will accelerate the development of flexible electronics [49].

When the flexible OFETs are manufactured in a large area, flexible electronic system will be improved dramatically, such as wearable electronic applications including foldable displays and medical sensors. Fukuda et al. [115] reported an organic TFT device exhibiting excellent mechanical stability and electrical characteristics. It was printed on ultra-flexible polymer films, achieving a high field-effect mobility of 1.0 $cm^2V^{-1}s^{-1}$ and a fast operating speed (∼ 1 ms) at low operating voltages. Moreover, the devices maintained operation under 50% compression without significant changes in their performance. In addition, they fabricated p-type diode-load inverter circuits easily on a large scale by the printing, which

functions well at low voltages and demonstrate good transfer characteristics. As Figure 7(b) (top) shows, the thickness of ultra-flexible organic devices is less than 2 μm and their weight is only 2 gm^{-2}. With these excellent properties, the devices conform to a human knee without any discomfort. Furthermore, the organic devices exhibited good robustness and demonstrate excellent stability in air, and at nominal temperatures and humidity though several stability tests. Figure 7(b) (middle) presents organic TFTs array printed on a flexible substrate over large areas and their electrical performance, including saturation mobility, threshold voltage and logarithmic on/off ratio. They could even conform to a human throat to provide a promising technique in health care. The unipolar diode-load inverters are fabricated on a thin parylene-C film, see Figure 7(b) (down) and have excellent static and dynamic electrical characteristics under 50% compression strain. The printed organic devices on large scale indicate a potential for application in flexible electronics such as foldable displays or medical sensors [115]. Tee et al. [34] presented a skin-inspired organic digital mechanoreceptor system. The system had three main components, as depicted in Figure 7(c) (top): flexible microstructured resistive pressure sensors with a high sensitivity, voltage-controlled oscillators fabricated by printed organic circuits, and a channelrhodopsin engineered specifically to enable optical neuron stimulation above 100 Hz (a range similar to that of slow-adapting mechanoreceptors). There were a series of studies about the sensing element. The initial idea was that a layer of elastomer, such as cross-linked poly (dimethylsiloxane), between two pieces of conductor to make a pressure sensor, but the sensitivity of the sensors was relatively low. To achieve excellent properties, microstructures and small air gaps were designed, such as using periodic structures of pyramids or lines. This kind of sensor could be easily compressed by a little pressure, which resulted in a large change in resistance. The sensor was sensitive to touch [116, 117].

The ring oscillator circuits were used to generate voltage spikes and consisted of odd numbers of repeating inverter stages based on complementary field-effect transistors through printing [118]. As Figure 7(c) (top) shows, the time delay of the oscillations was modulated by the pressure sensor as a component in a voltage divider. When the pressure increased, the supply voltage increased and the time delay of the transistors was reduced, leading to increasing the frequency of the oscillations. The whole process mimicked the slow-adapting mechanoreceptors. A model hand of DiTact sensors connected with stretchable silver nanowire conductors is shown in Figure 7(c) (middle). Besides they used mouse cortical neurons to demonstrate that neurons could be stimulated optically and electrically by the pressure-induced, frequency-modulated signal from the DiTact system, shown in Figure 7(c) (down). The system can be integrated in large scales as electronic skins for neural prosthetics or optogenetic-based prosthetic interfaces [34].

3.3 Flexible and organic lighting diode

Organic light-emitting diodes (OLED) operate via double injection luminescence. The electron and hole from cathode and anode, driven by an electric field, are injected into the organic electron transport layer and the organic hole transport layer. The recombination of the electron and hole yields excitons that relax to the ground state via radiative transition along with emitted light. Due to their low driving-voltage, low power consumption and flexible fabrication, OLEDs are all-solid thin-film luminescent devices that are promising for panel displays and wearable devices. We present the developments in structure designs for flexible OLEDs and the panel display devices.

Pei et al. [119] reported a flexible nanocomposite electrode comprising single-walled carbon nanotubes and silver nanowires stacked and embedded in the surface of a polymer substrate, as shown in Figure 8(a). Nanoparticles of barium strontium titanate were dispersed within the substrate to enhance light extraction efficiency, as shown in Figure 8(a) (left). Green polymer OLEDs (polymer light-emitting diodes (PLEDs), as Figure 8(a) (middle) shows) were fabricated on the nanocomposite electrode and exhibit a maximum current efficiency of 118 cdA^{-1} at 10000 cdm^{-2} with the calculated external quantum efficiency being 38.9%, as shown in Figure 8(a) (right). The efficiencies of white PLEDs are 46.7 cdA^{-1} and 30.5%, respectively. The experimentally obtained enhancement factor is 246% for green PLEDs and 224% for white PLEDs. The devices can be bent to a 3 mm radius repeatedly without significant loss of

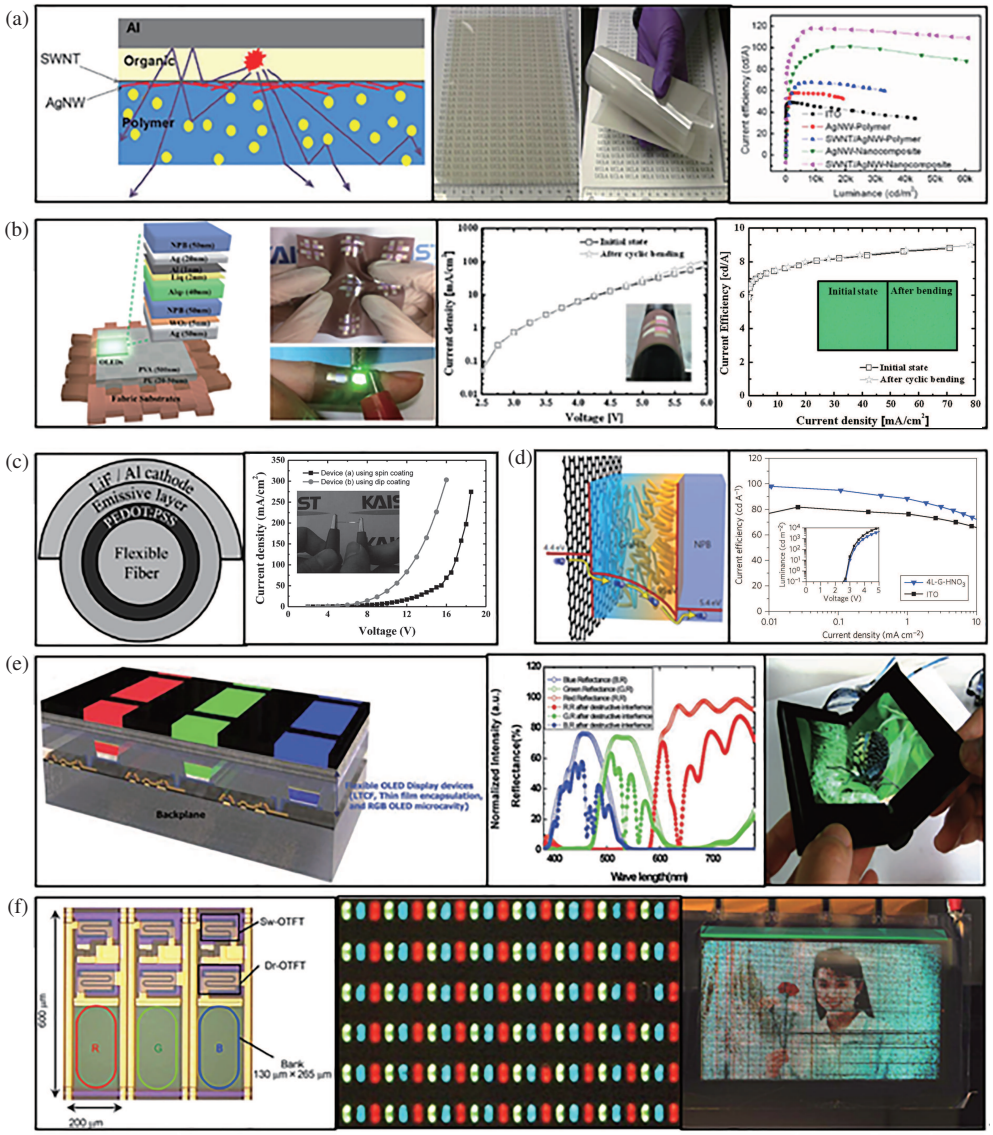

Figure 8 (Color online) (a) Schematic illustration of light scattering by nanoparticles in the SWNT/AgNW-nanocomposite (left), photographs of a nanocomposite film as prepared (middle), current efficiency-luminance (right) [119] @Copyright 2014 Springer Nature. (b) Schematic diagram of the cross-section of the planarized fabric substrates and the designed noninverted top-emitting OLEDs, photographs of the fabricated OLEDs when wrinkling the sample and operating the sample at 4.5 V (left), current density-voltage characteristics and bending image (middle), current efficiency-current density characteristics and optical microscope image of emitting cells operated at 5 mA/cm2 (right) [120] @Copyright 2013 Elsevier B.V. (c) PLED structures of devices using a fiber substrate (left) and a photograph of the fabricated device on a fiber substrate using the dip coating method (right) [79] @Copyright 2015 John Wiley and Sons. (d) Schematic illustration of a hole-injection process from a graphene anode via a self-organized HIL with work-function gradient (GraHIL) to the NPB layer (left), current efficiencies of phosphorescent OLED devices using 4L-G-HNO3 and ITO anodes (right) [121] @Copyright 2012 Springer Nature. (e) Cross-section diagram of the proposed flexible OLED display device composed of a LTCF, TFE, and a RGB OLED microcavity (left), the comparison of the measured data for the reflectance produced by only color filters and LTCFs with an OLED microcavity to verify the effect of a destructive interference of the microcavity (middle), optical image of a foldable/seamless OLED display (right) [24] @Copyright 2011 John Wiley and Sons. And (f) schematic top view of one pixel of flexible AMOLED display panel (left), photographs of electrophosphorescence from RGB subpixels of the display (middle) and display demonstration (right) [122] @Copyright 2012 John Wiley and Sons.

electroluminescent performance.

Kwon et al. [120] reported the first OLEDs on actual soft fabrics that can be used for a wearable display, as Figure 8(b) shows. Polyurethane (PU) and poly (vinyl alcohol) (PVA) layers, which only degrade slightly the flex stiffness of bare fabrics due to their ductile characteristics, were used as planarization

layers via a simple fabrication process involving lamination and spin-coating, as Figure 8(b) (left) shows. Therefore, many of the mechanical characteristics of the bare fabric substrates were retained in the planarized fabric substrates. The fabricated OLEDs on soft fabrics showed a high current efficiency of around 8 $\mathrm{cdA^{-1}}$ (Figure 8(b) (right)), reliability (Figure 8(b) (middle)) during a 1000 cycle bending test with a bending radius of 5 mm.

Kwon et al. [79] demonstrated PLEDs using the dip coating method on a flat glass and flat polyethylene terephthalate (PET) substrates as well as on a cylinder-shaped fiber substrate, as Figure 8(c) (left) shows. The fabricated PLEDs on glass substrates showed J-V-L characteristics similar to the control device fabricated using the spin coating method, as Figure 8(c) (right) shows. This result enables the production of low cost, easily fabricated flexible fiber-based PLEDs by roll-to-roll manufacturing as well as the realization of a true fiber-based wearable display.

To date, the luminous efficiency of OLEDs with graphene anodes has been limited by a lack of efficient methods to improve the low work function and reduce the sheet resistance of graphene films to the levels required for electrodes. Lee et al. [121] fabricated flexible OLEDs by modifying the graphene anode with their conducting polymer, which has a gradient work function, a high work function, and a low sheet resistance; thus they achieved extremely high luminous efficiencies, as Figure 8(d) shows. The highly efficient flexible phosphorescent green OLEDs showed much higher efficiencies (CE $\approx$ 98.1 $\mathrm{cdA^{-1}}$, LE $\approx$ 102.7 $\mathrm{lmW^{-1}}$) than those of the device with an ITO anode (81.8 $\mathrm{cdA^{-1}}$ and 85.60 $\mathrm{lmW^{-1}}$), as Figure 8(d) (right) shows. This approach demonstrates a way to increase device performance greatly by replacing ITO anodes with flexible graphene anodes in organic optoelectronic devices such as flexible, stretchable full-color displays and solid-state lighting.

Kim et al. [24] developed a flexible OLED display device having a top emission structure composed of an OLED microcavity covered with thin film encapsulation (TFE) and a low temperature color filter (LTCF), as Figure 8(e) (left) shows. LTCFs and a microcavity are utilized to reduce reflected light and thus enhance outdoor readability, where the primary wavelength was filtered by the LTCFs with a transmission factor of 70%–95%, and the destructive interferences of the OLED micro cavity reduce the overall reflectance to below 50%, as Figure 8(e) (middle) shows. The novel optical architecture, achieved contrast ratios of 14:1 at 500 lux and 150000:1 in dark ambient. Interestingly, the new optical system can lower the power consumption of the OLED panel by as much as 30%, compared to current OLED technology that utilizes polarization (POL) films. Figure 8(e) (right) shows an optical image of a foldable/seamless OLED display.

Suzuki et al. [122] fabricated a flexible phosphorescent color active-matrix organic light-emitting-diode (AMOLED) display on a plastic substrate driven by low-voltage organic thin-film-transistors (OTFTs), as shown in Figure 8(f). Phosphorescent RGB polymer layers were precisely patterned by ink-jet printing for OLEDs, as Figure 8(f) (middle) shows. An OTFT backplane with 42-ppi resolution, fabricated using pentacene, was used to drive the OLEDs. The OTFT exhibited a current on/off ratio of 106 and a mobility of 0.1 $\mathrm{cm^2V^{-1}s^{-1}}$, sufficient to drive the OLEDs. As Figure 8(f) (right) shows, the fabricated OLED display successfully showed moving color images at a field frequency of 60 Hz.

The aforementioned fabrication, of flexible OLEDs on unusual substrates of fabrics and fibers, could facilitate development of emerging applications such as wearable displays. In addition, the versatile OLEDs could also function as flexible displays when the reliability is sufficient for commercial use.

4 Flexible, stretchable and inorganic integrated electronics on large scale

The development, performance, and applications of traditional organic flexible electronics are limited by the characteristics of semiconductors. Organic electronics are flexible and stretchable with weak electrical properties, while inorganic electronics have better electrical properties but are brittle and easily destroyed. If inorganic electronics were to be flexible, the applications would increase manifold. This sections presents some types of inorganic, flexible, and stretchable electronic devices.

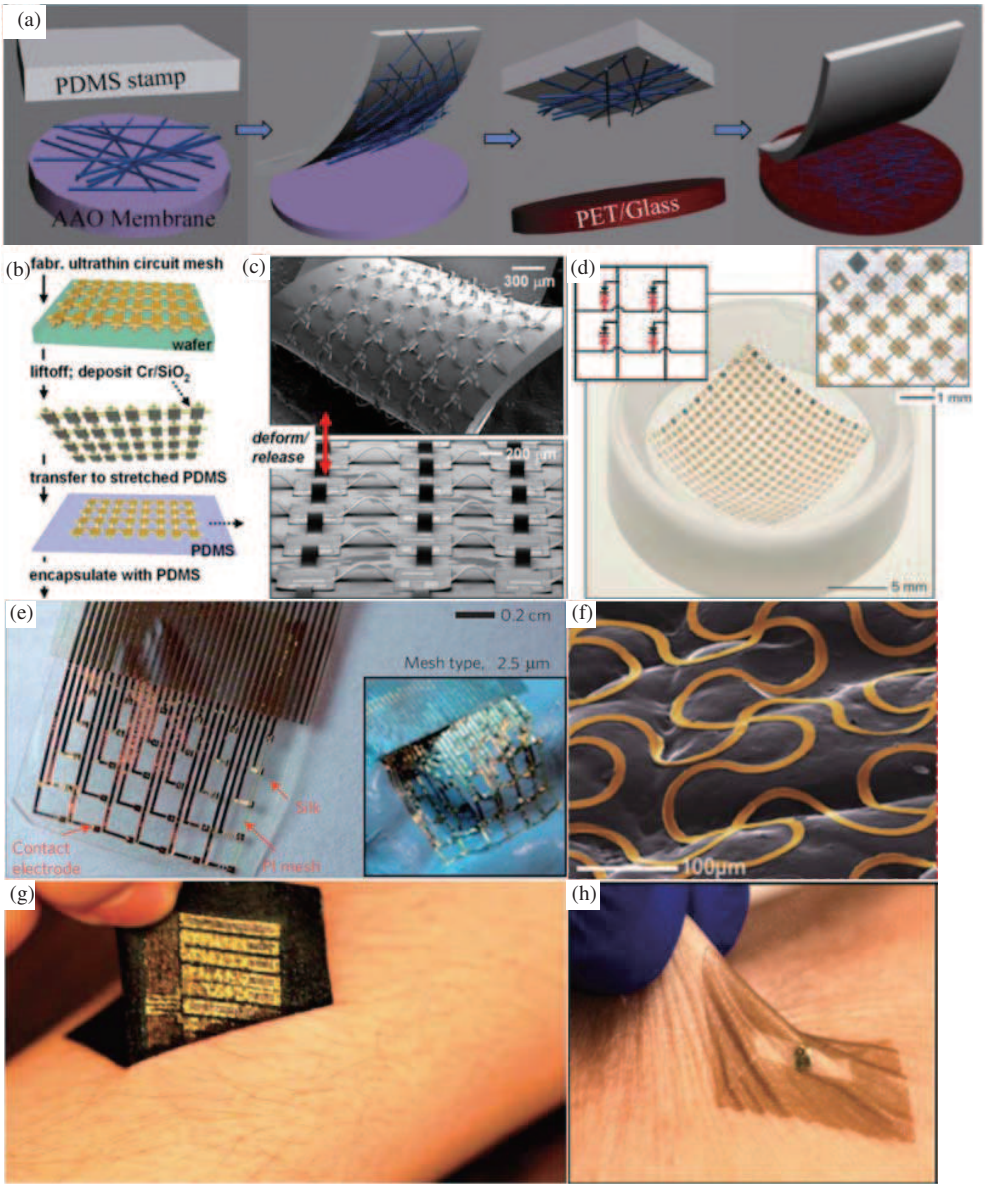

Figure 9 (Color online) (a) Schematic illustration of transfer process of conductive electrodes of silver nanowire films [123] @Copyright 2010, Springer Nature; (b) schematic illustration of fabrication process of high stretchability device [51] @Copyright 2008 National Academy of Sciences; (c) SEM image of an array of CMOS inverters [51] @Copyright 2008 National Academy of Sciences; (d) an array integrated on a hemispherical glass substrate [124] @Copyright 2008 Springer Nature; (e) an electrode array with a mesh design on a dissolvable silk substrate [125] @Copyright 2010 Springer Nature; (f) SEM image of a multifunctional electronics conformal contacting with the skin [126] @Copyright 2013 John Wiley and Sons; (g) peeling rugged and breathable forms of stretchable electronics off the skin [20] @Copyright 2014 Springer Nature; and (h) photo illustrates the conformity of a device for near-field communication [38] @Copyright 2014 John Wiley and Son.

4.1 Flexible, stretchable and inorganic circuits and devices

Manufacture of inorganic flexible integrated circuits often requires sophisticated methods, as well as the most high-performance materials. Certain materials and mechanical design strategies for classes of electronic circuits that offer extremely high stretchability, and enable accommodation of demanding configurations were introduced in 2008 [51].

Conductive electrodes of AgNW films using vacuum filtration and PDMS-assisted transfer printing on flexible substrates showd good mechanical flexibility [123]. Figure 9(a) shows the transfer process of the AgNW from an anodized aluminum oxide (AAO) membrane to the receiving substrate. The films

show good adhesion to the substrate, a low resistance of 10 Ωsq^{-1}, and have high quality with different line widths and shapes. Figure 9(b) shows a schematic overview of the fabrication of the circuits, where complementary metal-oxide-semiconductor (CMOS) circuits are defined on ultrathin plastic substrates and then transferred to stretched PDMS with thin Si wires which are only bonded at nodes [51]. Figure 9(c) shows SEM images of an array of CMOS inverters which show a high flexibility [51]. The use of single-crystal silicon nanomaterials for the semiconductor provides a performance in stretchable CMOS integrated circuits approaching that of conventional devices with comparable feature sizes formed on silicon wafers.

A hemispherical electronic eye camera using wafer-scale optoelectronics that was formed in unusual, two-dimensionally compressible configurations was introduced in 2008 [124]. Elastomeric transfer elements capable of transforming the planar layouts were initially fabricated into hemispherical geometries for their final implementation. Figure 9(d) shows the circuit diagram and an array integrated on a hemispherical glass. The method provided practical routes for integrating a planar device onto complex curvilinear objects, which is suitable for diverse applications. Figure 9(e) illustrates a material strategy for a type of bio-interfaced system that relies on ultrathin electronics supported by bioresorbable substrates of silk fibroin [125]. Specialized mesh designs and ultrathin forms for the electronics ensure minimal stresses on the tissue and highly conformal coverage, even for complex curvilinear surfaces, as confirmed by experimental and theoretical studies. Figure 9(f) shows a construct consisting of an interconnected collection of thin, filamentary serpentine conductive traces and integrated devices, all in an open mesh layout, which provided extremely low effective elastic moduli and large deformability, at the level of the overall system [126]. The sensors are capable of measuring electrophysiological (EP) signals, as seen in electrocardiograms (ECG) and electromyograms (EMG), as well as temperature and mechanical strain. Materials and composite designs for thin, breathable, soft electronics that can adhere strongly to the skin is illustrated in Figure 9(g) [20]. The device combines thin, ultralow modulus, cellular silicone materials with elastic, strain-limiting fabrics, to yield a compliant but rugged platform for stretchable electronics. The theoretical and experimental studies show the ability to be applied and removed hundreds of times without damaging the devices or the skin. The design could be used as cutaneous optical, electrical and radio frequency sensors for measuring hydration state, electrophysiological activity, pulse and cerebral oximetry. As Figure 9(h) shows, a materials and mechanics designs and integration strategies for near-field communication (NFC) is developed [38]. The device has the ability to accommodate large strain deformation with ultrathin, ultralow modulus electronics. The material and device architectures have potential for utility in other types of radio frequency (RF) electronic systems and for use on other organs of the body.

4.2 Flexible, stretchable and inorganic integrated sensors

High performance inorganic semiconductor materials gained flexibility and stretchability after structure and mechanics design as mentioned above. Metal oxide semiconductor field-effect transistors are one of the most typical examples of these electronics. As these inorganic flexible integrated circuits and sensors develop rapidly, wearable devices that could fit on a soft curved surface such as human skin would be of greater interest. These sensors are able to detect weak signals on human skin and transfer real-time signals for health monitoring.

Flexible electronics would play a significant role in the development of health monitoring devices since they can fit on human skin, making it easier to monitor physiological parameters such as blood pressure, blood glucose, and ECG. A platform that provides relevant quantitative data regarding surgical wound healing was developed in 2014 [127]. As Figure 10(a) (left and middle) shows, the platform consists two layers of silicone, two layers of polyimide and one layer of copper. As Figure 10(a) (right) shows, these kinds of thermal sensors and actuators could be used to provide temperature and thermal conductivity of the skin around the wounds for clinical studies. Skin-like devices could gather the dielectric properties and deformations of the skin [128]. From Figure 10(b) (left), excellent conformability and spontaneous integration and flexibility are clearly observed. A typical spectrum, as shown in Figure 10(b) (middle

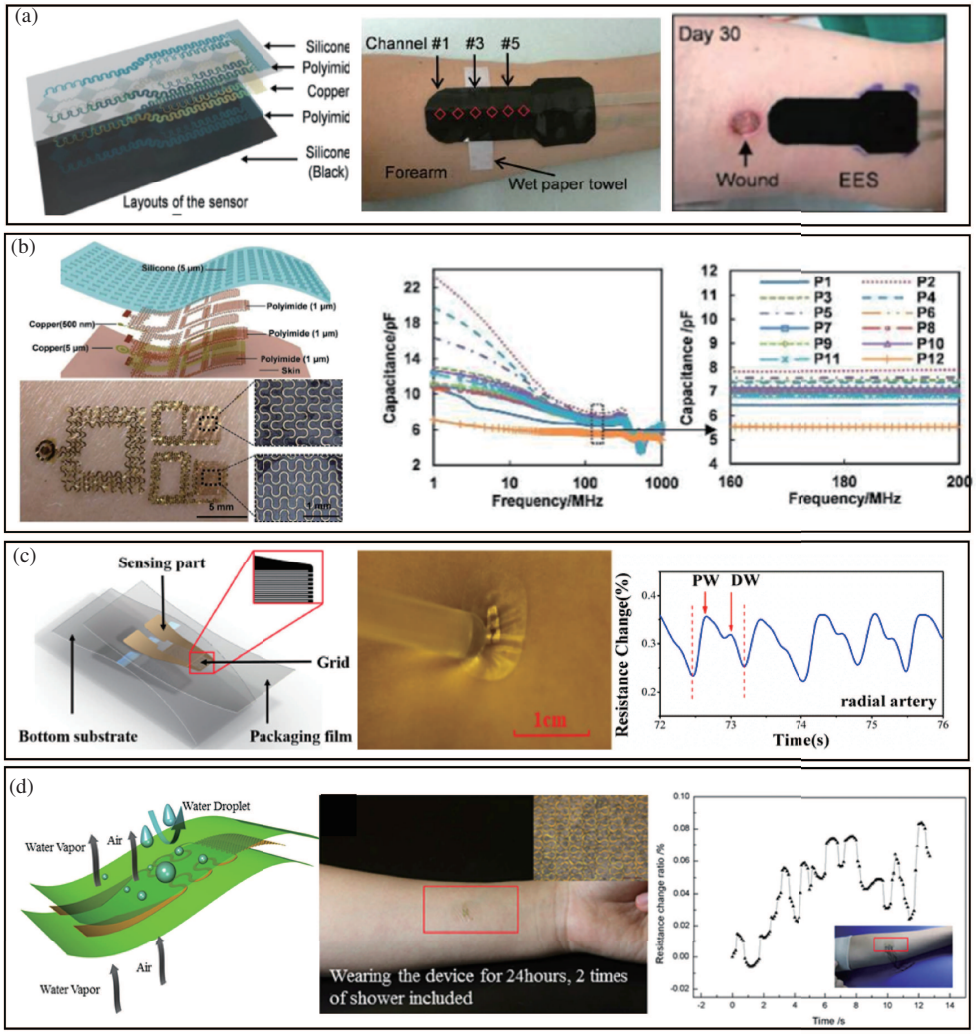

Figure 10 (Color online) (a) Device design (left) and schematic illustration (middle) of a device able to work on human wounds to provide data of surgical wound healing (right) [127] @Copyright 2014 John Wiley and Sons. (b) A multimodal wireless epidermal sensor. (left) Exploded view schematic diagram and images of the sensor on the skin. (middle) Representative variations in dielectric properties of the skin for frequencies between 1 MHz to 1 GHz, evaluated using a coaxial cable probe. (right) Minimal variations occur between 160 MHz to 200 MHz [128] @Copyright 2014 John Wiley and Sons. (c) Schematic diagram (left), images (middle) and experiment result of pulse wave from radial artery(right) of a flexible sensor on the skin [129] @Copyright 2016 IEEE. And (d) schematic illustration (left), images (middle) and Resistance change while the arm twisting and rotating (right) of water proof and vapor permeable property of flexible devices [130] @Copyright 2015 Springer Nature.

and right), measured with the coaxial cable exhibits a rapidly decreasing dielectric constant at low frequencies (from 1 to 90 MHz), followed by a more modest dependence at higher frequencies. The smallest dependence occurs in a range of frequencies from 160 to 200 MHz, where the capacitance varies by only $\approx 0.6\%$. Figure 10(c) shows a biocompatible and ultra-flexible strain sensor for long-term measurement of pulse and real-time body motion [129]. The sensor was integrated on a semipermeable substrate with good biocompatibility and waterproofness, showing better performance and higher precision in motion and pulse measurements than other similar sensors. A strategy for biocompatible flexible temperature sensors was proposed, inspired by skin and illustrated in Figure 10(d) (left and middle); this method possesses the excellent permeability of air and a high waterproof level by using a semipermeable film with porous structures as the substrate [130]. As Figure 10(d) (right) shows, an in vitro test shows no sign of maceration or stimulation to the skin. Other researchers [131] also demonstrated a soft, flexible device to perform mechano-acoustic recording from the skin on nearly every part of the body. Experiments showed

the application of seismocardiography and heart murmur detection in advanced clinical diagnostics.

4.3 Flexible, stretchable and inorganic integrated optoelectronics

Inorganic flexible integrated photoelectron circuits, which are optoelectronic devices integrated on flexible substrates, could expand the application of these devices in the field of medical treatment, solar cells and wearable devices. Light-emitting diode (LED) is a multipurpose and widely-applied illuminant with properties of high luminance, low energy consumption and long operational life span, which could be integrated onto a flexible substrate.

A process that uses commercially available electronic components and flip-chip bonding processes was conceived as a platform that can be used without modification to create stretchable electronic systems incorporating any set of electronic components [132]. As a demonstration, stretchable LED arrays containing up to 50 LEDs are fabricated and show that the arrays can survive repeated stretching of 90000 cycles and also tightly conform to a human thumb tip, as shown in Figure 11(a). Figure 11(b) illustrates a prototype of a flexible integrated photodetector system with rGO-based microsupercapacitor and a CdS nanowire-based photodetector [133]. The system showed reliable flexibility and stable photocurrent response, which is promising for large-scale and integrated photodetector circuits. Figure 11(c) demonstrates a skin-like flexible photonic device with colorimetric temperature indicators and wireless electronics to measure thermos on the skin [134]. The device also provided local heating by RF signals, while carrying out reactive hyperemia assessments of blood flow and hydration analysis. Adaptive flexible optoelectronic camouflage systems inspired from cephalopods visually adapting to their surroundings were presented, as Figure 11(d) (left and middle) shows, which could autonomously sense and adapt to the color of the environment [135]. The system consists of arrays of actuators and photodetectors to modulate the visual appearance of solid objects. Figure 11(d) (right) shows the simple pattern displayed on the devices while bent.

Optoelectronic devices usually exhibit accuracy in measuring physiological parameters by using characteristics of light: transmission, refraction, and reflection. 3D flexible elastic membranes shaped via 3D printing to precisely match the epicardium of the heart would make it able to capture the real-time status of the heart, as a platform for deformable arrays of multifunctional sensors, containing electronic and optoelectronic components [137]. Figure 11(e) illustrates a near-field wireless optoelectronics that is small, thin, and flexible, and could be implanted deep into the brain for optogenetics applications [136]. The overall construction of the device (Figure 11(e) (left)) was highlighting a freely adjustable needle with a μ-ILED at the tip end, connected to a receiver coil with matching capacitors, a rectifier, and a separate μ-ILED indicator. The device was very small and bendable (Figure 11(e) (middle)) and implanted into tissues (right) for optogenetics. A similar concept of flexible devices is being carried out by scientists with the optoelectronic functionality of obtaining blood oxygenation, as shown in Figure 11(f). Owing to the excellent flexibility and stretchability, this device conformed to skin (shown in Figure 11(f) (left and middle)) and measured SpO_2 and pulse rate [16].

4.4 Flexible, stretchable and inorganic integrated systems

The highly integrated systems of flexible sensors and devices mentioned above could have a variety of functions, such as signal detection, reception, processing, and transmission. Figure 12(a) illustrates materials and device design strategies for the core elements of wearable electronics, such as transistors, charge-trap floating-gate memory units, and various logic gates, with stretchable form factors [138]. The use of semiconducting carbon nanotube networks designed for integration with charge traps and ultrathin dielectric layers meets the performance requirements as well as reliability, proven by detailed material and electrical characterizations using statistics. Cardiology is always a hot topic in health monitoring and biomechanical energy harvesting. Figure 12(b) shows ultra-flexible piezoelectric devices integrated with the heart to harvest its biomechanical energy [97]. Figure 12(b) (middle) shows a strategy for energy harvesting from heart motion by using a ultra-flexible piezoelectric device based on lead zirconate titanate (PZT) ceramics to light LEDs (Figure 12(b) (right)), without any burden or damage to hearts.

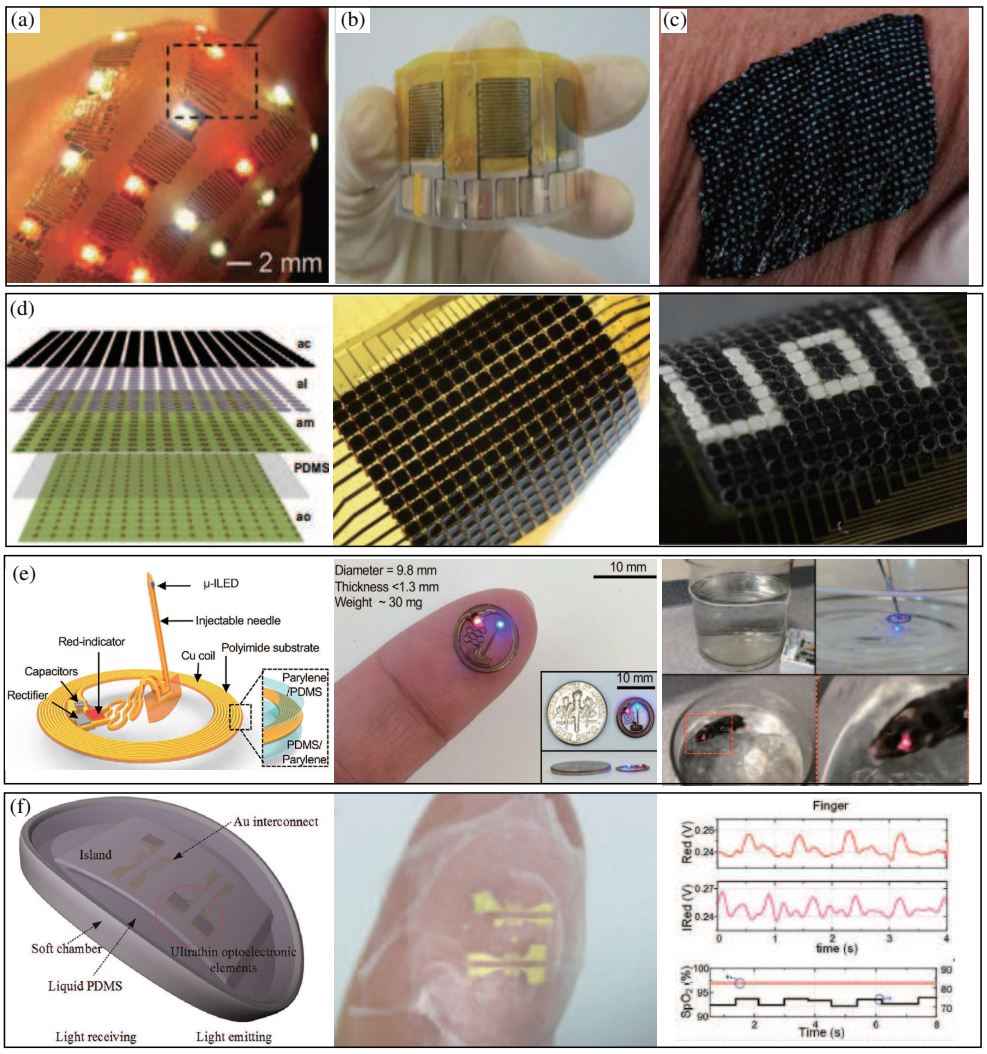

Figure 11 (Color online) (a) A flexible LED arrays wrapped on a human thumb [132] @Copyright 2011 John Wiley and Sons. (b) A microsupercapacitor used for photo detector system [133] @Copyright 2015 Elsevier Ltd. All rights reserved. (c) Skin-like flexible photonic device with colorimetric temperature indicators deformed in a twisting motion [134] @Copyright 2014 Springer Nature. (d) The schematic diagram (left) and images (middle) of adaptive flexible optoelectronic camouflage systems. The simple pattern displayed on the devices while bent (right) [135] @Copyright 2014 National Academy of Sciences. (e) Schematic diagram (left) and images (middle) of a near-field wireless optoelectronics device. Images of water tank with single-loop antenna, working devices under the water, and a swimming mouse that has a working device (right) [136] @Copyright 2016 Elsevier Inc. (f) Schematic diagram (left), images (middle) of epidermal optoelectronic devices and SpO2 and pulse rate (right) [16] @Copyright 2017 John Wiley and Sons.

Flexible integrated systems could be used in long-term cardiac electrophysiology in Figure 12(c) [139]. The capacitive coupled arrays integrated on ultrathin dielectric layer which could protect the underlying electronics from biological fluids (as Figure 12(c) (left and middle) shows) show good high current-leakage level and long operational lifetimes and were able to realize long-term ECG detection (Figure 12(c) (right)).

On the other hand, flexible, stretchable and inorganic integrated systems on the skin for human treatment and diagnosing are promising. Figure 12(d) shows a low modulus compliant system with multiple chip-scale electrical components using three-dimensional architectures instead of traditional two-dimensional layouts to obtain electrophysiological recordings [140]. With helical microcoils the 3D interconnected networks show exceptional low modulus and elastic mechanics, and was able to reach the required sophisticated level of functionality. Figure 12(e) demonstrates a skin-like biosensor system with paper battery-powered electrochemical twin channels for noninvasive, in situ, and highly accurate in-

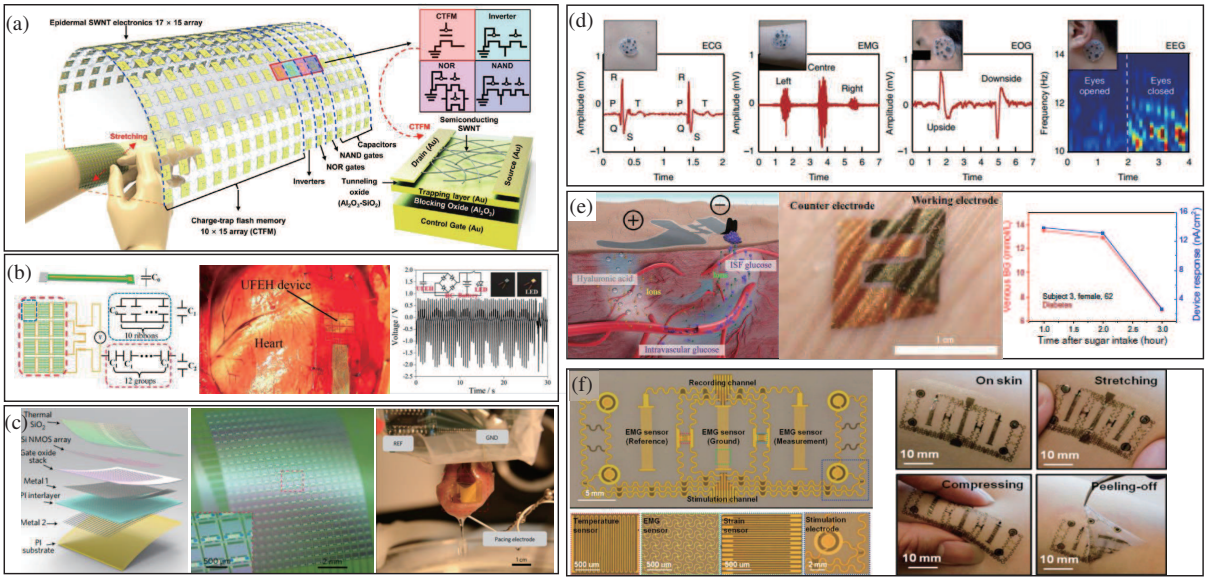

Figure 12 (Color online) (a) Schematic illustration of an integrated wearable platform based on s-SWNT [138] @Copyright 2015 American Chemical Society. (b) (left) Electrical connecting sketch of device. (middle) Image of device when the heart relaxes in diastoles. (right) Output voltage measured by AD/DA card [97] @Copyright 2015 Springer Nature. (c) An exploded-view schematic (left, highlighting the key functional layers) and a photograph (middle) of a completed capacitively coupled flexible sensing system with 396 nodes in a slightly bent state. (right) A photograph of a flexible capacitively coupled sensing electronic system on a Langendorff-perfused rabbit heart [139] @Copyright 2017 Springer Nature. (d) Electrophysiological recordings with inset images of the low modulus compliant system on the skin: electrocardiogram (ECG), electromyogram (EMG), electrooculogram (EOG) and electroencephalogram (EEG) [140] @Copyright 2017 Springer Nature. (e) (left) Schematic of blood glucose monitoring system on-skin. (middle) The biosensor completely conforms to the skin surface. (right) Results of blood glucose measured by using a plasma blood test with a vein detained needle (red) and blood glucose monitoring system on-skin (blue) during the OGTT [17]. And (f) (left) planar view optical image of multifunctional device with skin-like physical characteristics and capabilities in both sensing and stimulation. (right) Images of a device mounted on the forearm, with examples under stretching, compressing, and peeling-off [39] @Copyright 2015 John Wiley and Sons.

travascular blood glucose monitoring [17]. The designed subcutaneous ETCs (Figure 12(e) (left) and (middle)) drive intravascular blood glucose out of the vessel and transport it to the skin surface for being measured (Figure 12(e) (right)). Figure 12(f) [39] illustrates a system of neuromuscular electrical stimulation with sensors for electromyography, temperature and mechanical strain, which allows acquisition of physiological data, and neural stimulatory inputs, and the ability to activate electrical muscle.

5 Conclusion and outlooks

In this review, recent progress in fabrication strategies of flexible electronics, and large-scale organic-inorganic flexible electronic systems are systematically summarized. Organic and inorganic flexible electronics have advantages and disadvantages.

Flexible and organic electronics. Advantages: (1) With the organic semiconductor materials, organic electronics are flexible in the absence of mechanical design. (2) With advanced fabrication strategies, flexible and organic electronics are low-cost and able to be fabricated on large scale. (3) Using organic material, they are ultrathin and ultra-lightweight. (4) With new organic semiconductor materials, novel devices can be created. Disadvantages: (1) Compared to inorganic semiconductor devices, flexible and organic electronics have weak electrical properties, such as low electron mobility and electric conductivity. (2) The mechanical properties and electrical properties of the devices can be degraded easily, when the devices is bent and stretched. (3) The properties of organic electronics are not always stable.

Flexible, stretchable and inorganic electronics. Advantages: (1) Because of semiconductor

materials, inorganic electronics offer high electric efficiency and long service life. (2) With 2D and 3D buckling design, stretchable and inorganic electronics have the capacity to absorb large levels of strain. (3) Benefiting from the development of traditional semiconductor devices, inorganic electronics have the mature fabrication method, such as epitaxial growth. Disadvantages: (1) Flexible, stretchable and inorganic electronics are intrinsically brittle at a device level, owing to the fragile characteristic of semiconductor material. (2) There is no suitable fabrication method for large-scale integration of flexible, stretchable and inorganic electronics.

Comparing the advantages of flexible and organic electronics to flexible and inorganic electronics, we confirm that the organic and inorganic flexible electronics complement each other. By combining these two types of flexible electronics and novel strategies of organic-inorganic hybrid integration, flexible electronics will enhance many applications further.

With the acceleration of social information, further integration of information and humans will likely continue. Once the various devices acting as information carriers achieve flexibility, electronics will essentially promote the efficient interaction of people and information. Flexible electronics are most likely to achieve breakthroughs in the field of medical devices. With the continuous innovation and advancement of integrated circuits and biomedicine, the treatment of cardiovascular diseases, diabetes and neurological diseases that threaten the aging population and the sub-health population, there will be increasing reliance on implantable medical electronics. With the improvement of medical treatment, these implantable medical devices will have greater degrees of association with the corresponding tissues and organs, which requires the medical electronics to be more flexible and more suitable for the structure of flexible tissues and organs. This demand is further driving the development of flexible, implantable medical electronics, such as wireless cardiac monitoring devices attached to the heart, real-time cerebrovascular monitoring devices, and so on. With the demand of medical diagnosis and treatment, flexible electronics will flourish rapidly. In all cases, fundamental developments in existing and new flexible electronics, including growth techniques, assembly methods, composite designs, processing strategies, structure/property relationships, integration schemes, and mechanical/electrical/optical properties will determine the rate of progress.

Acknowledgements This work was supported by National Basic Research Program of China (973) (Grant No. 2015CB351904) and National Natural Science Foundation of China (Grant Nos. 11625207, 11320101001, 11227801).

References

1 Zardetto V, Brown T M, Reale A, et al. Substrates for flexible electronics: a practical investigation on the electrical, film flexibility, optical, temperature, and solvent resistance properties. J Polym Sci B Polym Phys, 2011, 49: 638–648
2 Someya T, Sekitani T, Iba S, et al. A large-area, flexible pressure sensor matrix with organic field-effect transistors for artificial skin applications. Proc Natl Acad Sci USA, 2004, 101: 9966–9970
3 Yoon J, Baca A J, Park S I, et al. Ultrathin silicon solar microcells for semitransparent, mechanically flexible and microconcentrator module designs. Nat Mater, 2008, 7: 907–915
4 Ahn J H, Kim H S, Lee K J, et al. Heterogeneous three-dimensional electronics by use of printed semiconductor nanomaterials. Science, 2006, 314: 1754–1757
5 Kaltenbrunner M, Sekitani T, Reeder J, et al. An ultra-lightweight design for imperceptible plastic electronics. Nature, 2013, 499: 458–463
6 Someya T, Bao Z, Malliaras G G. The rise of plastic bioelectronics. Nature, 2016, 540: 379–385
7 Kim D H, Lu N, Ma R, et al. Epidermal electronics. Science, 2011, 333: 838–843
8 Park S I, Ahn J H, Feng X, et al. Theoretical and experimental studies of bending of inorganic electronic materials on plastic substrates. Adv Funct Mater, 2008, 18: 2673–2684
9 Feng X, Yang B D, Liu Y, et al. Stretchable ferroelectric nanoribbons with wavy configurations on elastomeric substrates. ACS Nano, 2011, 5: 3326–3332
10 Wang Y, Chen Y, Li H, et al. Buckling-based method for measuring the strain-photonic coupling effect of GaAs nanoribbons. ACS Nano, 2016, 10: 8199–8206
11 Imani S, Bandodkar A J, Mohan A V, et al. A wearable chemical-electrophysiological hybrid biosensing system for real-time health and fitness monitoring. Nat Commun, 2016, 7: 11650

12 Schwartz G, Tee B C K, Mei J, et al. Flexible polymer transistors with high pressure sensitivity for application in electronic skin and health monitoring. Nat Commun, 2013, 4: 1859

13 Gao W, Emaminejad S, Nyein H Y Y, et al. Fully integrated wearable sensor arrays for multiplexed in situ perspiration analysis. Nature, 2016, 529: 509–514

14 Lee H, Choi T K, Lee Y B, et al. A graphene-based electrochemical device with thermoresponsive microneedles for diabetes monitoring and therapy. Nat Nanotech, 2016, 11: 566–572

15 Koh A, Kang D, Xue Y, et al. A soft, wearable microfluidic device for the capture, storage, and colorimetric sensing of sweat. Science Transl Medicine, 2016, 8: 165

16 Li H, Xu Y, Li X, et al. Epidermal inorganic optoelectronics for blood oxygen measurement. Advanced Healthc Mater, 2017, 6: 1601013

17 Chen Y, Lu S, Zhang S, et al. Skin-like biosensor system via electrochemical channels for noninvasive blood glucose monitoring. Sci Adv, 2017, 3: e1701629

18 Webb R C, Ma Y, Krishnan S, et al. Epidermal devices for noninvasive, precise, and continuous mapping of macrovascular and microvascular blood flow. Sci Adv, 2015, 1: e1500701–e1500701

19 Yokota T, Zalar P, Kaltenbrunner M, et al. Ultraflexible organic photonic skin. Sci Adv, 2016, 2: e1501856–e1501856

20 Jang K I, Han S Y, Xu S, et al. Rugged and breathable forms of stretchable electronics with adherent composite substrates for transcutaneous monitoring. Nat Commun, 2014, 5: 4779

21 Lee C H, Ma Y, Jang K I, et al. Soft core/shell packages for stretchable electronics. Adv Funct Mater, 2015, 25: 3698–3704

22 Sekitani T, Nakajima H, Maeda H, et al. Stretchable active-matrix organic light-emitting diode display using printable elastic conductors. Nat Mater, 2009, 8: 494–499

23 Chen J L, Liu C T. Technology advances in flexible displays and substrates. IEEE Access, 2013, 1: 150–158

24 Kim S, Kwon H J, Lee S, et al. Low-power flexible organic light-emitting diode display device. Adv Mater, 2011, 23: 3511–3516

25 Rogers J A, Bao Z, Baldwin K, et al. From the cover: paper-like electronic displays: large-area rubber-stamped plastic sheets of electronics and microencapsulated electrophoretic inks. Proc Natl Acad Sci USA, 2001, 98: 4835–4840

26 Kim D H, Lu N, Ghaffari R, et al. Materials for multifunctional balloon catheters with capabilities in cardiac electrophysiological mapping and ablation therapy. Nat Mater, 2011, 10: 316–323

27 Lee C H, Kim H, Harburg D V, et al. Biological lipid membranes for on-demand, wireless drug delivery from thin, bioresorbable electronic implants. NPG Asia Mater, 2015, 7: e227

28 Briseno A L, Tseng R J, Ling M M, et al. High-performance organic single-crystal transistors on flexible substrates. Adv Mater, 2006, 18: 2320–2324

29 Khang D Y, Jiang H, Huang Y, et al. A stretchable form of single-crystal silicon for high-performance electronics on rubber substrates. Science, 2006, 311: 208–212

30 Reuss R H, Chalamala B R, Moussessian A, et al. Macroelectronics: perspectives on technology and applications. Proc IEEE, 2005, 93: 1239–1256

31 Chiang C K, Fincher Jr C, Park Y W, et al. Electrical conductivity in doped polyacetylene. Phys Rev Lett, 1977, 39: 1098–1101

32 Tsumura A, Koezuka H, Ando T. Macromolecular electronic device: field-effect transistor with a polythiophene thin film. Appl Phys Lett, 1986, 49: 1210–1212

33 Forrest S R. The path to ubiquitous and low-cost organic electronic appliances on plastic. Nature, 2004, 428: 911–918

34 Tee B C K, Chortos A, Berndt A, et al. A skin-inspired organic digital mechanoreceptor. Science, 2015, 350: 313–316

35 Park K S, Baek J, Park Y, et al. Inkjet-assisted nanotransfer printing for large-scale integrated nanopatterns of various single-crystal organic materials. Adv Mater, 2016, 28: 2874–2880

36 Kumagai S, Murakami H, Tsuzuku K, et al. Solution-processed organic-inorganic hybrid CMOS inverter exhibiting a high gain reaching 890. Org Electron, 2017, 48: 127–131

37 Sun Y, Choi W M, Jiang H, et al. Controlled buckling of semiconductor nanoribbons for stretchable electronics. Nat Nanotech, 2006, 1: 201–207

38 Kim J, Banks A, Cheng H, et al. Epidermal electronics with advanced capabilities in near-field communication. Small, 2015, 11: 906–912

39 Xu B, Akhtar A, Liu Y, et al. An epidermal stimulation and sensing platform for sensorimotor prosthetic control, management of lower back exertion, and electrical muscle activation. Adv Mater, 2016, 28: 4462–4471

40 Xu R, Lee J W, Pan T, et al. Designing thin, ultrastretchable electronics with stacked circuits and elastomeric encapsulation materials. Adv Funct Mater, 2017, 27: 1604545

41 Tang C W, VanSlyke S A. Organic electroluminescent diodes. Appl Phys Lett, 1987, 51: 913–915

42 Hoofman R J O M, de Haas M P, Siebbeles L D A, et al. Highly mobile electrons and holes on isolated chains of the

semiconducting polymer poly(phenylene vinylene). Nature, 1998, 392: 54–56
43 Afzali A, Dimitrakopoulos C D, Breen T L. High-performance, solution-processed organic thin film transistors from a novel pentacene precursor. J Am Chem Soc, 2002, 124: 8812–8813
44 Horowitz G, Peng X Z, Fichou D, et al. Role of the semiconductor/insulator interface in the characteristics of π-conjugated-oligomer-based thin-film transistors. Synth Met, 1992, 51: 419–424
45 Kawasaki N, Kalb W L, Mathis T, et al. Flexible picene thin film field-effect transistors with parylene gate dielectric and their physical properties. Appl Phys Lett, 2010, 96: 113305
46 Park Y, Han K S, Lee B H, et al. High performance n-type organic-inorganic nanohybrid semiconductors for flexible electronic devices. Org Electron, 2011, 12: 348–352
47 Gburek B, Wagner V. Influence of the semiconductor thickness on the charge carrier mobility in P3HT organic field-effect transistors in top-gate architecture on flexible substrates. Org Electron, 2010, 11: 814–819
48 Uno M, Nakayama K, Soeda J, et al. High-speed flexible organic field-effect transistors with a 3D structure. Adv Mater, 2011, 23: 3047–3051
49 Min S Y, Kim T S, Kim B J, et al. Large-scale organic nanowire lithography and electronics. Nat Commun, 2013, 4: 1773
50 Ahn J H, Kim H S, Menard E, et al. Bendable integrated circuits on plastic substrates by use of printed ribbons of single-crystalline silicon. Appl Phys Lett, 2007, 90: 213501
51 Kim D H, Song J, Choi W M, et al. From the cover: materials and noncoplanar mesh designs for integrated circuits with linear elastic responses to extreme mechanical deformations. Proc Natl Acad Sci USA, 2008, 105: 18675–18680
52 Ko H C, Shin G, Wang S, et al. Curvilinear electronics formed using silicon membrane circuits and elastomeric transfer elements. Small, 2009, 5: 2703–2709
53 Kim D H, Xiao J, Song J, et al. Stretchable, curvilinear electronics based on inorganic materials. Adv Mater, 2010, 22: 2108–2124
54 Ma Y, Feng X, Rogers J A, et al. Design and application of 'J-shaped' stress-strain behavior in stretchable electronics: a review. Lab Chip, 2017, 17: 1689–1704
55 Meitl M A, Zhu Z T, Kumar V, et al. Transfer printing by kinetic control of adhesion to an elastomeric stamp. Nat Mater, 2006, 5: 33–38
56 Baca A J, Ahn J H, Sun Y, et al. Semiconductor wires and ribbons for high-performance flexible electronics. Angew Chem Int Ed, 2008, 47: 5524–5542
57 Feng X, Meitl M A, Bowen A M, et al. Competing fracture in kinetically controlled transfer printing. Langmuir, 2007, 23: 12555–12560
58 Kim S, Wu J, Carlson A, et al. Microstructured elastomeric surfaces with reversible adhesion and examples of their use in deterministic assembly by transfer printing. Proc Natl Acad Sci USA, 2010, 107: 17095–17100
59 Huang Y, Zheng N, Cheng Z, et al. Direct laser writing-based programmable transfer printing via bioinspired shape memory reversible adhesive. ACS Appl Mater Interfaces, 2016, 8: 35628–35633
60 Chen H, Feng X, Huang Y, et al. Experiments and viscoelastic analysis of peel test with patterned strips for applications to transfer printing. J Mech Phys Solids, 2013, 61: 1737–1752
61 Cai S, Zhang C, Li H, et al. Surface evolution and stability transition of silicon wafer subjected to nano-diamond grinding. AIP Adv, 2017, 7: 035221
62 Thorsen T, Maerkl S J, Quake S R. Microfluidic large-scale integration. Science, 2002, 298: 580–584
63 Zhang L, Di C-a, Yu G, et al. Solution processed organic field-effect transistors and their application in printed logic circuits. J Mater Chem, 2010, 20: 7059–7073
64 Mishra A, Bäuerle P. Small molecule organic semiconductors on the move: promises for future solar energy technology. Angew Chem Int Ed, 2012, 51: 2020–2067
65 Lin P, Yan F. Organic thin-film transistors for chemical and biological sensing. Adv Mater, 2012, 24: 34–51
66 Wang C H, Hsieh C Y, Hwang J C. Flexible organic thin-film transistors with silk fibroin as the gate dielectric. Adv Mater, 2011, 23: 1630–1634
67 Bettinger C J, Becerril H A, Kim D H, et al. Microfluidic arrays for rapid characterization of organic thin-film transistor performance. Adv Mater, 2011, 23: 1257–1261
68 Knopfmacher O, Hammock M L, Appleton A L, et al. Highly stable organic polymer field-effect transistor sensor for selective detection in the marine environment. Nat Commun, 2014, 5: 2954
69 Pandey M, Pandey S S, Nagamatsu S, et al. Solvent driven performance in thin floating-films of PBTTT for organic field effect transistor: role of macroscopic orientation. Org Electron, 2017, 43: 240–246
70 Soeda J, Matsui H, Okamoto T, et al. Highly oriented polymer semiconductor films compressed at the surface of ionic liquids for high-performance polymeric organic field-effect transistors. Adv Mater, 2014, 26: 6430–6435
71 McCulloch I, Heeney M, Bailey C, et al. Liquid-crystalline semiconducting polymers with high charge-carrier mobility.

Nat Mater, 2006, 5: 328–333
72 Park J U, Hardy M, Kang S J, et al. High-resolution electrohydrodynamic jet printing. Nat Mater, 2007, 6: 782–789
73 Lee S, Moon G D, Jeong U. Continuous production of uniform poly(3-hexylthiophene) (P3HT) nanofibers by electrospinning and their electrical properties. J Mater Chem, 2009, 19: 743–748
74 Liu H, Reccius C H, Craighead H G. Single electrospun regioregular poly(3-hexylthiophene) nanofiber field-effect transistor. Appl Phys Lett, 2005, 87: 253106
75 Singh M, Haverinen H M, Dhagat P, et al. Inkjet printing-process and its applications. Adv Mater, 2010, 22: 673–685
76 Hwang J K, Cho S, Dang J M, et al. Direct nanoprinting by liquid-bridge-mediated nanotransfer moulding. Nat Nanotech, 2010, 5: 742–748
77 Liang J, Tong K, Pei Q. A water-based silver-nanowire screen-print ink for the fabrication of stretchable conductors and wearable thin-film transistors. Adv Mater, 2016, 28: 5986–5996
78 Moonen P F, Yakimets I, Huskens J. Fabrication of transistors on flexible substrates: from mass-printing to high-resolution alternative lithography strategies. Adv Mater, 2012, 24: 5526–5541
79 Kwon S, Kim W, Kim H C, et al. P-148: polymer light-emitting diodes using the dip coating method on flexible fiber substrates for wearable displays. SID Symposium Digest Technical Papers, 2015, 46: 1753–1755
80 Søndergaard R, Hösel M, Angmo D, et al. Roll-to-roll fabrication of polymer solar cells. Mater Today, 2012, 15: 36–49
81 Hyun W J, Secor E B, Hersam M C, et al. High-resolution patterning of graphene by screen printing with a silicon stencil for highly flexible printed electronics. Adv Mater, 2015, 27: 109–115
82 Krebs F C, Alstrup J, Spanggaard H, et al. Production of large-area polymer solar cells by industrial silk screen printing, lifetime considerations and lamination with polyethyleneterephthalate. Sol Energy Mater Sol Cells, 2004, 83: 293–300
83 Qin D, Xia Y, Whitesides G M. Soft lithography for micro- and nanoscale patterning. Nat Protoc, 2010, 5: 491–502
84 Kumar A, Whitesides G M. Features of gold having micrometer to centimeter dimensions can be formed through a combination of stamping with an elastomeric stamp and an alkanethiol "ink" followed by chemical etching. Appl Phys Lett, 1993, 63: 2002–2004
85 Xia Y, McClelland J J, Gupta R, et al. Replica molding using polymeric materials: a practical step toward nanomanufacturing. Adv Mater, 1997, 9: 147–149
86 Zhao X M, Xia Y, Whitesides G M. Fabrication of three-dimensional micro-structures: microtransfer molding. Adv Mater, 1996, 8: 837–840
87 Perl A, Reinhoudt D N, Huskens J. Microcontact printing: limitations and achievements. Adv Mater, 2009, 21: 2257–2268
88 Kooy N, Rahman N, Mohamed K. Patterning of multi-leveled microstructures on flexible polymer substrate using roll-to-roll ultraviolet nanoimprint lithography. In: Prcoeedings of the 35th IEEE/CPMT International Electronics Manufacturing Technology Conference (IEMT), Ipoh, 2012. 1–5
89 Chou S Y, Krauss P R, Renstrom P J. Imprint of sub-25 nm vias and trenches in polymers. Appl Phys Lett, 1995, 67: 3114–3116
90 Haisma J, Verheijen M, Heuvel K V D, et al. Mold-assisted nanolithography: a process for reliable pattern replication. J Vac Sci Technol B, 1996, 14: 4124–4128
91 Ahn S H, Guo L J. Large-area roll-to-roll and roll-to-plate nanoimprint lithography: a step toward high-throughput application of continuous nanoimprinting. ACS Nano, 2009, 3: 2304–2310
92 Meitl M A, Zhu Z T, Kumar V, et al. Transfer printing by kinetic control of adhesion to an elastomeric stamp. Nat Mater, 2005, 5: 33–38
93 Menard E, Meitl M A, Sun Y G, et al. Micro- and nanopatterning techniques for organic electronic and optoelectronic systems. Chem Rev, 2007, 107: 1117–1160
94 Baughman R H, Zakhidov A A, de Heer W A. Carbon nanotubes–the route toward applications. Science, 2002, 297: 787–792
95 Björk P, Holmström S, Inganäs O. Soft lithographic printing of patterns of stretched DNA and DNA/electronic polymer wires by surface-energy modification and transfer. Small, 2006, 2: 1068–1074
96 Smythe E J, Dickey M D, Whitesides G M, et al. A technique to transfer metallic nanoscale patterns to small and non-planar surfaces. ACS Nano, 2009, 3: 59–65
97 Lu B W, Chen Y, Ou D P, et al. Ultra-flexible piezoelectric devices integrated with heart to harvest the biomechanical energy. Sci Rep, 2015, 5: 16065
98 Dagdeviren C, Yang B D, Su Y, et al. Conformal piezoelectric energy harvesting and storage from motions of the heart, lung, and diaphragm. Proc Natl Acad Sci USA, 2014, 111: 1927–1932
99 Park S I, Xiong Y, Kim R H, et al. Printed assemblies of inorganic light-emitting diodes for deformable and semi-

transparent displays. Science, 2009, 325: 977–981
100 Kim D H, Ahn J H, Choi W M, et al. Stretchable and foldable silicon integrated circuits. Science, 2008, 320: 507–511
101 Saeidpourazar R, Li R, Li Y, et al. Laser-driven micro transfer placement of prefabricated microstructures. J Microelectromech Syst, 2012, 21: 1049–1058
102 Eisenhaure J D, Sang I R, Al-Okaily A A M, et al. The use of shape memory polymers for microassembly by transfer printing. J Microelectromech Syst, 2014, 23: 1012–1014
103 Reese C, Roberts M, Ling M M, et al. Organic thin film transistors. Mater Today, 2004, 7: 20–27
104 Bettinger C J, Bao Z. Organic thin-film transistors fabricated on resorbable biomaterial substrates. Adv Mater, 2010, 22: 651–655
105 Klauk H, Halik M, Zschieschang U, et al. Flexible organic complementary circuits. IEEE Trans Electron Devices, 2005, 52: 618–622
106 Jung Y H, Chang T H, Zhang H, et al. High-performance green flexible electronics based on biodegradable cellulose nanofibril paper. Nat Commun, 2015, 6: 7170
107 Grimsdale A C, Leok Chan K, Martin R E, et al. Synthesis of light-emitting conjugated polymers for applications in electroluminescent devices. Chem Rev, 2009, 109: 897–1091
108 Roberts M E, Sokolov A N, Bao Z. Material and device considerations for organic thin-film transistor sensors. J Mater Chem, 2009, 19: 3351–3363
109 Thompson B C, Fréchet J M J. Polymer-fullerene composite solar cells. Angew Chem Int Ed, 2008, 47: 58–77
110 Zhou L, Wanga A, Wu S C, et al. All-organic active matrix flexible display. Appl Phys Lett, 2006, 88: 083502
111 Mei J, Kim D H, Ayzner A L, et al. Siloxane-terminated solubilizing side chains: bringing conjugated polymer backbones closer and boosting hole mobilities in thin-film transistors. J Am Chem Soc, 2011, 133: 20130–20133
112 Sun S, Lan L, Xiao P, et al. Flexible organic field-effect transistors with high-reliability gate insulators prepared by a room-temperature, electrochemical-oxidation process. RSC Adv, 2015, 5: 15695–15699
113 Lee B H, Hsu B B, Patel S N, et al. Flexible organic transistors with controlled nanomorphology. Nano Lett, 2015, 16: 314–319
114 Kelley T W, Muyres D V, Baude P F, et al. High performance organic thin film transistors. MRS Online Proceedings Library Archive, 2003, 771: 169–179
115 Fukuda K, Takeda Y, Yoshimura Y, et al. Fully-printed high-performance organic thin-film transistors and circuitry on one-micron-thick polymer films. Nat Commun, 2014, 5: 4147
116 Mannsfeld S C B, Tee B C K, Stoltenberg R M, et al. Highly sensitive flexible pressure sensors with microstructured rubber dielectric layers. Nat Mater, 2010, 9: 859–864
117 Tee B C K, Chortos A, Dunn R R, et al. Tunable flexible pressure sensors using microstructured elastomer geometries for intuitive electronics. Adv Funct Mater, 2014, 24: 5427–5434
118 Sekitani T, Yokota T, Zschieschang U, et al. Organic nonvolatile memory transistors for flexible sensor arrays. Science, 2009, 326: 1516–1519
119 Liang J, Li L, Pei Q, et al. A solution processed flexible nanocomposite electrode with efficient light extraction for organic light emitting diodes. Sci Rep, 2014, 4: 4307
120 Kim W, Kwon S, Lee S M, et al. Soft fabric-based flexible organic light-emitting diodes. Org Electron Phys Mater Appl, 2013, 14: 3007–3013
121 Han T H, Lee Y, Choi M R, et al. Extremely efficient flexible organic light-emitting diodes with modified graphene anode. Nat Photon, 2012, 6: 105–110
122 Suzuki M, Fukagawa H, Nakajima Y, et al. A 5.8–in. phosphorescent color AMOLED display fabricated by ink-jet printing on plastic substrate. J Soc Inf Display, 2012, 17: 1037–1042
123 Madaria A R, Kumar A, Ishikawa F N, et al. Uniform, highly conductive, and patterned transparent films of a percolating silver nanowire network on rigid and flexible substrates using a dry transfer technique. Nano Res, 2010, 3: 564–573
124 Ko H C, Stoykovich M P, Song J, et al. A hemispherical electronic eye camera based on compressible silicon optoelectronics. Nature, 2008, 454: 748–753
125 Kim D H, Viventi J, Amsden J J, et al. Dissolvable films of silk fibroin for ultrathin conformal bio-integrated electronics. Nat Mater, 2010, 9: 511–517
126 Yeo W H, Kim Y S, Lee J, et al. Multifunctional epidermal electronics printed directly onto the skin. Adv Mater, 2013, 25: 2773–2778
127 Hattori Y, Falgout L, Lee W, et al. Multifunctional skin-like electronics for quantitative, clinical monitoring of cutaneous wound healing. Adv Healthcare Mater, 2014, 3: 1597–1607
128 Huang X, Liu Y, Cheng H, et al. Materials and designs for wireless epidermal sensors of hydration and strain. Adv Funct Mater, 2014, 24: 3846–3854

129 Chen Y, Lu B, Chen Y, et al. Biocompatible and ultra-flexible inorganic strain sensors attached to skin for long-term vital signs monitoring. IEEE Electron Device Lett, 2016, 37: 496–499
130 Chen Y, Lu B, Chen Y, et al. Breathable and stretchable temperature sensors inspired by skin. Sci Rep, 2015, 5: 11505
131 Liu Y, Norton J J S, Qazi R, et al. Epidermal mechano-acoustic sensing electronics for cardiovascular diagnostics and human-machine interfaces. Sci Adv, 2016, 2: e1601185–e1601185
132 Hu X, Krull P, de Graff B, et al. Stretchable inorganic-semiconductor electronic systems. Adv Mater, 2011, 23: 2933–2936
133 Xu J, Shen G. A flexible integrated photodetector system driven by on-chip microsupercapacitors. Nano Energy, 2015, 13: 131–139
134 Gao L, Zhang Y, Malyarchuk V, et al. Epidermal photonic devices for quantitative imaging of temperature and thermal transport characteristics of the skin. Nat Commun, 2014, 5: 4938
135 Yu C, Li Y, Zhang X, et al. Adaptive optoelectronic camouflage systems with designs inspired by cephalopod skins. Proc Natl Acad Sci USA, 2014, 111: 12998–13003
136 Shin G, Gomez A M, Al-Hasani R, et al. Flexible near-field wireless optoelectronics as subdermal implants for broad applications in optogenetics. Neuron, 2017, 93: 509–521.e3
137 Xu L, Gutbrod S R, Bonifas A P, et al. 3D multifunctional integumentary membranes for spatiotemporal cardiac measurements and stimulation across the entire epicardium. Nat Commun, 2014, 5: 3329
138 Son D, Koo J H, Song J K, et al. Stretchable carbon nanotube charge-trap floating-gate memory and logic devices for wearable electronics. ACS Nano, 2015, 9: 5585–5593
139 Fang H, Yu K J, Gloschat C, et al. Capacitively coupled arrays of multiplexed flexible silicon transistors for long-term cardiac electrophysiology. Nat Biomed Eng, 2017, 1: 0038
140 Jang K I, Li K, Chung H U, et al. Self-assembled three dimensional network designs for soft electronics. Nat Commun, 2017, 8: 15894